

# Regressive-transgressive cyclothem with facies record of the re-flooding window in the Late Silurian carbonate succession (Podolia, Ukraine)

PIOTR ŁUCZYŃSKI, WOJCIECH KOZŁOWSKI, STANISŁAW SKOMPSKI

*Institute of Geology, University of Warsaw, Al. Żwirki i Wigury 93; PL-02-089 Warszawa, Poland.  
E-mails: Piotr.Luczynski@uw.edu.pl, Wojciech.Kozlowski@uw.edu.pl, Skompski@uw.edu.pl*

## ABSTRACT:

Łuczynski, P., Kozłowski, W. and Skompski, S. 2015. Regressive-transgressive cyclothem with facies record of the re-flooding window in the Late Silurian carbonate succession (Podolia, Ukraine). *Acta Geologica Polonica*, **65** (3), 297–318. Warszawa.

The term “re-flooding window” was recently proposed as a time-interval connected with the transgressive stage of present day peri-reefal development. In the analysis presented here, a fossil record of a re-flooding window has been recognized. Nine Late Silurian carbonate sections exposed on the banks of the Dnister River in Podolia (Ukraine) have been correlated base on bed-by-bed microfacies analysis and spectral gamma ray (SGR) measurements. Correlated were sections representing settings ranging from the inner part of a shallow-water carbonate platform to its slope, through an organic buildup. The reconstructed depositional scenario has been divided into six development stages, with the first three representing a regressive interval and the latter three a transgressive interval of the basin’s history. The re-flooding window has been identified at the beginning of a transgressive part of the succession. Surprisingly, it is characterized by an extremely fast growth of a shallow, tide-dominated platform and by deposition of calciturbiditic layers in a more basinal area. The interpreted succession is a small-scale model illustrating the reaction of carbonate depositional sub-environments to sea level changes and determining the facies position of the stromatoporoid buildups within the facies pattern on a Silurian shelf. The use of SGR analyses in shallow water, partly high-energy, carbonate facies, both for correlation purposes and for identifying depositional systems, is a relatively new method, and thus can serve as a reference for other studies of similar facies assortment.

**Keywords:** Re-flooding window; Spectral gamma ray record; Shallow water carbonates; Late Silurian; Podolia.

## INTRODUCTION

In the Silurian the SW margin of the Baltica continent was occupied by a carbonate ramp, with the deposition governed by eustatic sea level changes. The eustatic pattern is recorded by a cyclic succession of carbonate deposits stretching from western Ukraine, through Belarus, Poland, Lithuania, Latvia, Estonia, central part of the Baltic Sea, up to Scania in southern

Sweden. The reconstructed facies array is usually presented as a set of belts (Text-fig. 1A), running more or less parallel to the shoreline, with a central zone of shallows (barriers?) dominated by stromatoporoid-coral buildups separating the outer shelf areas from inner shelf lagoons (Kaljo 1970; Nestor and Einasto 1997; Tuuling and Flodén 2011). The morphology and origin of these buildups remains dubious. In most areas, the Silurian is covered by younger deposits and

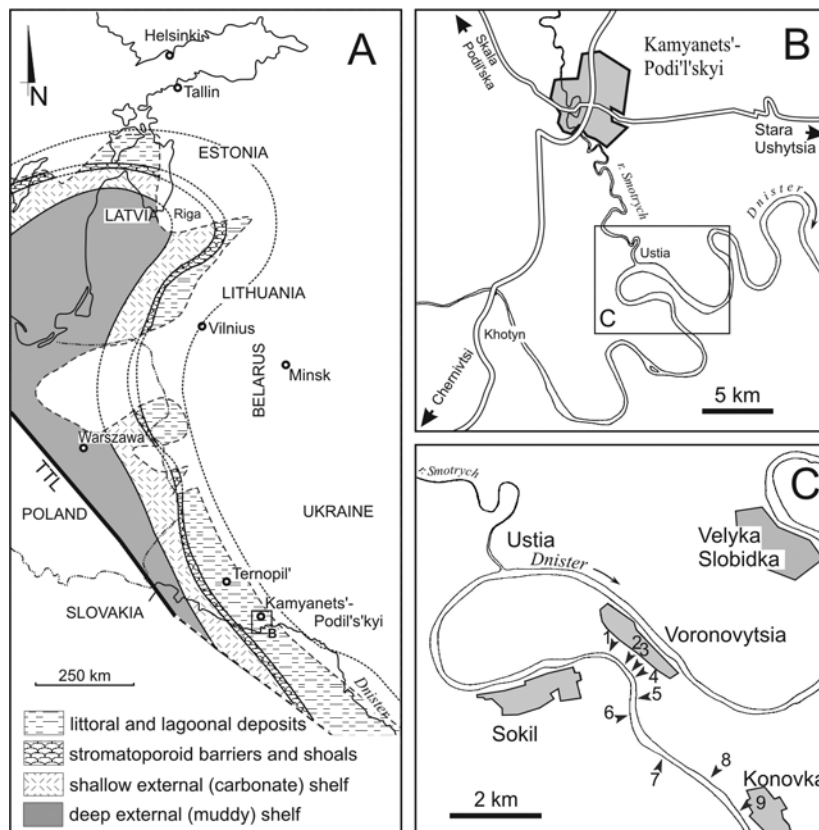
the reconstruction of the course of particular facies belts is based mainly on boreholes (e.g., Kaljo 1977).

The most thoroughly studied parts of the shelf are the Silurian exposures on Gotland and in the Glint zone in the Baltic States. The localities on Gotland yield numerous sedimentological data that allow tracing the evolution of the succession through time (Mantten 1971; Laufeld and Bassett 1981; Cherns 1983; Samtleben *et al.* 2000; Baarli *et al.* 2003). However, in spite of good exposures, the Gotland sections do not enable study of the anatomy of a carbonate platform in detail and for a selected time horizon, and particularly give no opportunity to reconstruct lateral facies changes. This results from a substantial tectonic tilting of the layers, which is combined with relatively shallow erosional cuts and with a general lack of sections perpendicular to the facies zones. Therefore, the reconstructions of facies patterns in the area are based mainly on seismic profiles analyses (e.g., Flodén *et al.* 2001; Bjerkéus and Eriksson 2001), and the resulting models are effects of their interpretations.

An attempt at creating a facies model of the Silurian carbonate shelf on Baltica has also been made in the Baltic States. Numerous boreholes penetrating the

whole area that were drilled during the last century enabled reconstruction of the general pattern of carbonate facies on the shelf (Nestor and Einasto 1977) and allowed listing a catalogue of organisms dwelling in particular zones (Einasto *et al.* 1986). However, the resulting models, based mainly on Walther's principle, contain no information on spatial relations between isochronous facies, and on the lateral width of particular zones. Moreover, large distances between individual boreholes make it necessary to interpolate the obtained data between scattered observation points.

In this context, the complete Silurian succession of Podolia exposed on the banks of Dnister and its left tributaries gives a unique opportunity to verify the proposed models and to examine the nature of variously developed stromatoporoid beds. Our earlier studies (Skompski *et al.* 2008; Łuczyński *et al.* 2009, 2014) have revealed that part of these beds, particularly those in the higher part of the Silurian succession, are in fact represented by sediments composed of material redeposited shoreward and derived from open marine regions. One can assume that some of the stromatoporoid biostromes on Gotland are of a similar origin (compare, Kershaw 1990).



Text-fig. 1. Location of the study area. A – Distribution of Upper Silurian facies along the margin of the East European Craton (after Einasto *et al.*, 1986, simplified); B – Location of the study area; C – Location of sections studied: 1 – Voronovtsia north, 2 – Voronovtsia forereef, 3 – Voronovtsia reef, 4 – Voronovtsia backreef, 5 – Voronovtsia south, 6 – Sokil north, 7 – Sokil south, 8 – Konovka quarry, 9 – Konovka village

The original accumulations of massive stromatoporoids, which were the source of the bioclastic material, are poorly recognized in terms of their morphological form and the ecological role played by particular organisms (Nestor and Einasto 1997; Munnecke 2007; Kershaw *et al.* 2007; Hubmann and Suttner 2007). This is in spite of the fact that observations can be made on both Silurian and Devonian stromatoporoid buildups around the world. The succession interpreted in the present work, which embraces only a small fragment of the Malynivtsi "Formation", can be treated as a small-scale model illustrating the two issues listed below:

- (i) reaction of carbonate depositional sub-environments to sea level changes,
- (ii) facies position of the stromatoporoid buildups within the facies pattern on a Silurian shelf.

#### GENERAL SETTING

The Silurian succession of Podolia is exposed on high banks of the Dnister River, between its left side Ternava tributary on the east, and the village of Dnistrove on the west, where a parastratotype of the Silurian/Devonian boundary is located. Due to a slight westward dip of the strata, four consecutive complexes: Kytaigorod, Bahovytsia, Malynivtsi and Skala crop out along the river (Tsegelnjuk *et al.* 1983; Nikiforova *et al.* 1972; Drygant 1984; Koren' *et al.* 1989; Kaljo *et al.* 2007). The complexes can be treated as "para-formations" – units corresponding to formations, but never properly defined in their formal sense. The lower part of the Malynivtsi "Formation" is the Konovka "Subformation" (Text-fig. 2), with maximum thickness of up to 25 metres. Its upper portion (Shutnivtsi "Member") embraces the main part of the investigated sections cropping out along both banks of the Dnister, between the villages of Konovka and Voronovytsia, south of Kamyanyets' Podil's'kyj<sup>1</sup> (Text-figs 1B, C and 3A).

A nodular limestone complex in the uppermost part of the sections corresponds to the Sokil "Member" of the Tsviklivtsi "Subformation" (Text-fig. 2).

The Konovka "Subformation" embraces two main lithotypes, classified by Tsegelnjuk *et al.* (1983) as Goloskiv and Shutnivtsi subsuites ("Members"). The lower of them is represented by open marine nodular limestones dominated by an *Atrypella linguata* brachiopod assemblage, accompanied by ostracods, gastropods, rugose corals and bivalve accumulations. In its upper part, the brachiopod assemblage becomes more diverse

and the fauna is enriched by more common occurrence of tabulate corals, bryozoans and sporadically also by tentaculitids. The lithotype contains also relatively common *Zoophycos* trace fossils and monospecific accumulations of *Atrypa reticularis* or *Protochonetes ludlowiensis*. According to Tsegelnjuk *et al.* (1983), the nodular limestones of this subsuite interfinger with stromatoporoid-coral-algal bioherms. Predtechensky *et al.* (1983, outcrops 25, 26A, 32, 204, 205 therein) based on both lithology and faunal assemblage (compare, Gritsenko *et al.* 1999) interpreted the nodular limestones as deposits of an open but shallow shelf.

The upper subsuite is usually developed as massive limestones, but in the vicinity of Sokil and Konovka it is facially replaced by dolomitic deposits, usually yellowish, with desiccation cracks, devoid of sessile benthic fauna and dominated by rare occurrences of ostracods of the *Tollitia-Amygdaella-Beyrichia* assemblage. The dolomitic complex most probably accumulated in lagoonal settings (Abushik and Evdokimova 1999). The occurrence of lagoonal deposits in the upper part of the Konovka "Subformation" inclined Predtechensky *et al.* (1983) to interpret the whole complex as regressive.

The observation polygon is small and embraces only an interval a dozen or so metres thick that can be traced laterally over a distance of about 4 km (Text-fig. 1B, C); nonetheless the succession encompasses a complete regressive-transgressive cycle. The represented sub-environments include a stromatoporoid bioherm and the adjacent facies from both the sea- and the shore sides. Of particular interest in the succession is the transition from the regressive to the transgressive stage, with well-preserved intervals of rapid acceleration of sedimentation (catch-up stage *sensu* Neumann and Macintyre 1985). An important advantage of the model is that it is represented by a wide array of facies, ranging from shallow water peritidal dolomites to open marine nodular limestones. Its shortcomings lie in the poor accessibility to the bioherm and in the general lack of biostratigraphical correlation lines. Although, within particular exposures located on the same bank of Dnister, the neighbouring sections could be correlated more or less precisely bed-by-bed, the same could not be done for exposures located on the opposite riverbanks.

Chronostratigraphically the investigated succession corresponds to the lower part of Ludfordian (Tsegelnjuk *et al.* 1983; compare, Racki *et al.* 2012). The broader context of the spatially complicated facies relationships in the interval investigated has been discussed by Predtechensky *et al.* (1983, fig. 3, sections no 32, 204, 205).

<sup>1</sup> All Ukrainian geographical names, as well as names of lithostratigraphical units, are transliterated into the Latin alphabet according to a conventional system for romanizing Ukrainian proper names into English

Epoch	Stage	Lithostratigraphy		Cyclothem		
		"Formation"	"Member"	meso- deep	shallow	macro-
Ludlow	Ludfordian	Malynivtsi	Rykhta	Isakivtsi	[shaded area]	[shaded area]
				Grintchuk		
			Tsviklivtsi	Bernove		
				Sokil		
			Konovka	Shutnivtsi		
	Gorsian	Bahovytsia		Goloskiv	[shaded area]	[shaded area]
				Ustia		
				Muksha		

Text-fig. 2. Simplified stratigraphical scheme of the Podolian Ludlow; lithostratigraphy and chronostratigraphical correlation according to Tsegelnjuk *et al.* 1983; Drygant 1983; Koren *et al.* 1989; Racki *et al.* 2012; cyclothem interpretation after Predtechensky *et al.* 1983. Stratigraphic position of the studied sections indicated by shadow bar

## METHODS

The basic method used to characterize lithology and facies development was classic macro- and microfacies analysis. In addition, field gamma ray measurements have been made throughout the sections, using a portable Gamma Surveyor GMS/CN gamma ray spectrometer (GF Instruments, Czech Republic). Complex application of facies analysis and gamma ray measurements allowed presenting a sedimentation scenario in a sequence stratigraphic context.

The total gamma signal commonly simply duplicates the macroscopically visible lithological changes. However, measured values of particular components of the total signal, coming from potassium, thorium and uranium, enabled the identification of several correlation horizons that can be interpreted as isochronous. Quantitative relations of some components, especially the Th/K ratio and the biogenic uranium content ( $U_{\text{bio}}$ ) are of great importance for palaeoenvironmental interpretations.

Three-minute long measurements were performed on flat extensive rock surfaces, away from the bends in the cliffs. Radiometrically determined abundances of potassium, thorium and uranium (eK, eTh, eU) were used for calculations of the Th/K ratio and the biogenic uranium content ( $U_{\text{bio}} = U - \text{Th}/3$ ; after Lüning and Kolonic 2003). Additionally, the potassium content, which strictly correlates with the total gamma signal, has been used in further analyses.

The natural gamma radiation of sedimentary rocks is derived from unstable isotopes of a decay chain of

potassium ( $^{40}\text{K}$ ), thorium ( $^{232}\text{Th}$ ) and uranium ( $^{238}\text{U}$ ). Individual isotopes generate gamma radiation with a strictly specified energy and hence the natural gamma spectrometric measurements allow determination of the concentration of parent nuclides. Potassium, thorium and uranium have different geochemical behaviours in the diastrophic cycle (Adams and Weaver 1958) and are concentrated in various rock-forming minerals (e.g., Dypvik and Eriksen 1983; Hesselbo 1996). Hence, the interpretation of the spectral gamma record always depends on the general lithology and the mineralogical composition.

In the case of the marly limestones and dolomites, the natural gamma ray signal is strongly dominated by potassium, which correlates very well with the total gamma intensity. The potassium content in carbonates is related to the abundance of the clay component (mainly illite), which in shallow carbonate environments reflects the energy level during sedimentation. Vertical changes of this parameter have a low potential for lateral correlations, simply because it is strongly influenced by the bottom relief. However, in cases of widely observed distinct facies changes resulting from sea-level fluctuations, the potassium content can be used to define some guide horizons.

The two most important SGR (spectral gamma ray) geochemical parameters in this study are the Th/K ratio and the calculated biogenic U content ( $U_{\text{bio}}$ ).

Thorium and uranium have similar ion radiuses and both are concentrated in the final phases of the magmatic processes (Ragland *et al.* 1967), rarely forming their own mineral phases. In endogenic processes, the Th/U ratio increases during magmatic differentiation, and hence it is an important proxy in provenance analysis (McLennan *et al.* 1993). During exogenic processes the thorium remains immobile and is concentrated in the duricrust as Th-bearing, clay mineral size grains of primary or secondary rare minerals (rhabdophane, florencite; Du *et al.* 2012), often absorbed into residual clays (Durrance 1986). At the same time, the uranium is leached from the solid phase of the sediment, which results in a gradual increase of the Th/U ratio (Carpentier *et al.* 2013).

During exposure of carbonate platforms, similar preservation of thorium and uranium is expected. Due to a generally low content of both elements in pure carbonates and their relatively higher concentration in terrigenous impurities, both elements are often over-concentrated in residual clays as related to the source rocks (Gu *et al.* 2013), even despite the preferential diminution of some of the uranium that is incorporated into the organic matter (Spirakis 1996) and the soluble phase. Later evolution of the weathering cover is ex-

pected to be similar to that in clastic rocks, or in weathered profiles developed on magmatic rocks. In these cases, longer exposure to weathering factors causes residual enrichment in thorium (Galan *et al.* 2007; Fernandez-Caliani and Cantano 2010), along with progressive diminution of uranium (Feng 2011; Carpentier *et al.* 2013). During exposure, thorium can also be supplied from external sources, e.g. by wind, which may additionally increase its concentration (Feng 2011). In the case of development of thicker weathering profiles, the thorium and uranium concentrated in the clay fraction accumulate in deeper horizons (Taboada *et al.* 2006), which protects the Th-bearing insoluble phases from mechanical washing out into the basin. On exposed carbonate platforms, a shallow position of the groundwater level usually does not allow deeper illuviation of the Th-bearing clay material.

According to the assumptions listed above, the increase of thorium content in carbonate sediments is influenced mainly by the supply of terrigenous components. As thorium occurs mainly in the clay fraction, its concentration in terrigenous impurities in carbonates can be monitored by the Th/K ratio, which reflects the dissection rate of the weathering profiles and their relative maturation. On the other hand, the overall changes of clay mineral composition may also modify the Th/K ratio by enrichment or depletion of the K-rich component (illite). Independently of the dominant affecting factor, the Th/K ratio seems to be useful for at least short distance correlation in carbonate successions, as a proxy of thorium concentration in the terrigenous component and/or of overall changes in the clay mineral composition.

Another proxy used in the present study is the calculated biogenic uranium content ( $U_{\text{bio}}$ ). As a redox-sensitive trace element, in most cases uranium shows good correlation with the TOC – total organic carbon (Lüning and Kolonic 2003), and its enrichment often marks levels of sedimentary condensation or enhanced bioproductivity. However, due to a general uranium impoverishment in carbonate-dominated sedimentary environments, the uranium supplied with the terrigenous components may constitute an important or even a dominant part of its total content, and thus an adequate correction for determining the share of the biogenic component ( $U_{\text{bio}}=U\cdot\text{Th}/3$ ) is needed (Lüning and Kolonic 2003). The calculated biogenic uranium content can be interpreted as a proxy of sedimentation rate, with its maxima marking condensation levels coinciding with flooding events, or sediment starvation events.

## LITHOFACIES CHARACTERISTICS OF THE COMPLEXES

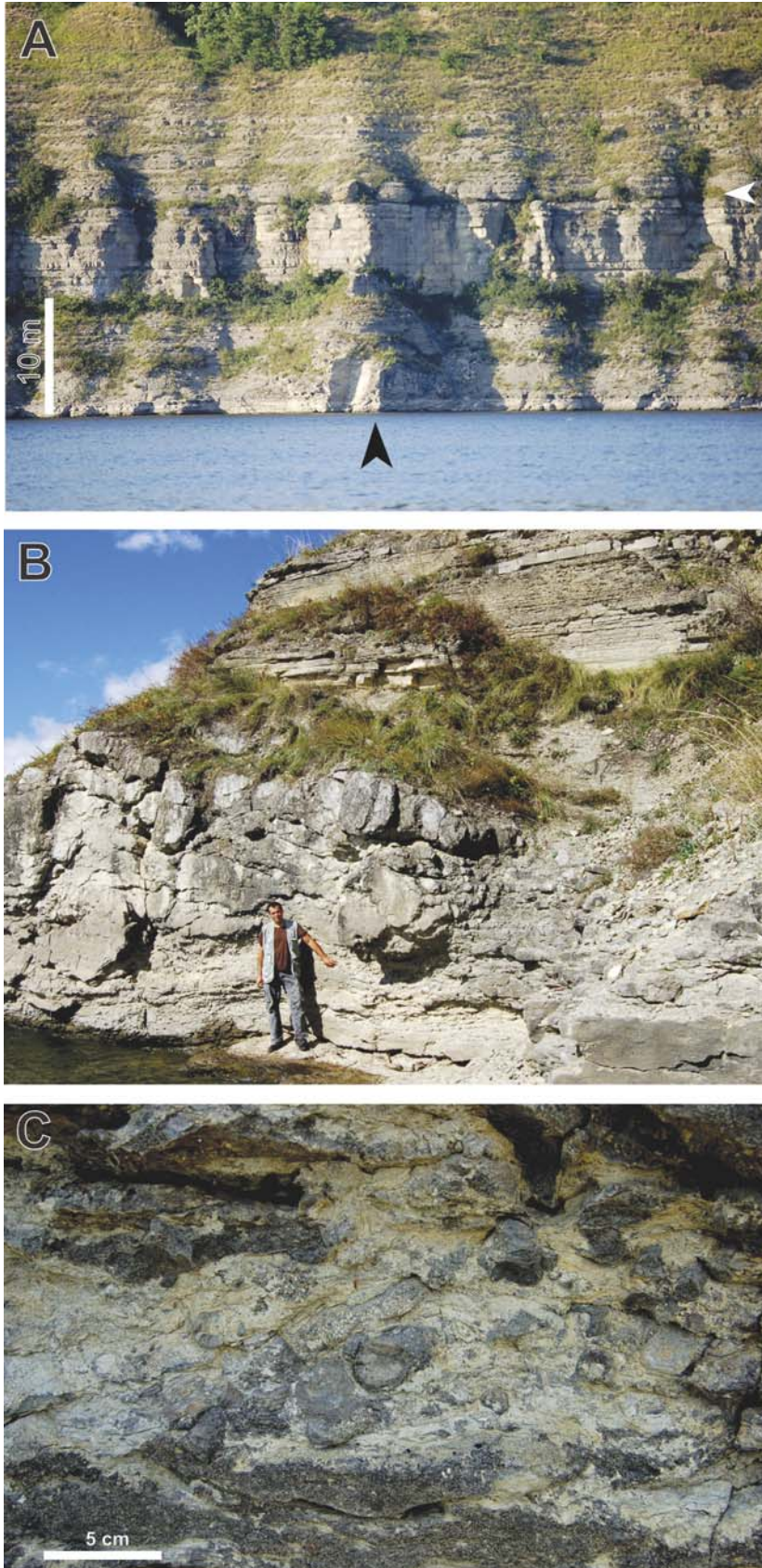
The macroscopically most conspicuous lithotype of the analysed sections are the laminated dolomitic beds, characterized by a whole array of horizontal and wavy laminae. In most of the sections (apart from the Voronovytzia north section (1)) the dolomitic complex separates the lower and the upper parts of the lithological succession. Results of gamma ray measurements and the analysis of its components allow treating the lower boundary of the dolomites as an isochrone, and therefore on correlation sections it is drawn as a main reference line (Text-fig. 4). All units exposed below this line are here referred to as the lower part of the succession, and those exposed above as the upper part of the succession. The described complexes are treated here as lithological-genetic units and therefore facies interpretations are presented as an integral part of their characteristics.

### Lower part of the succession

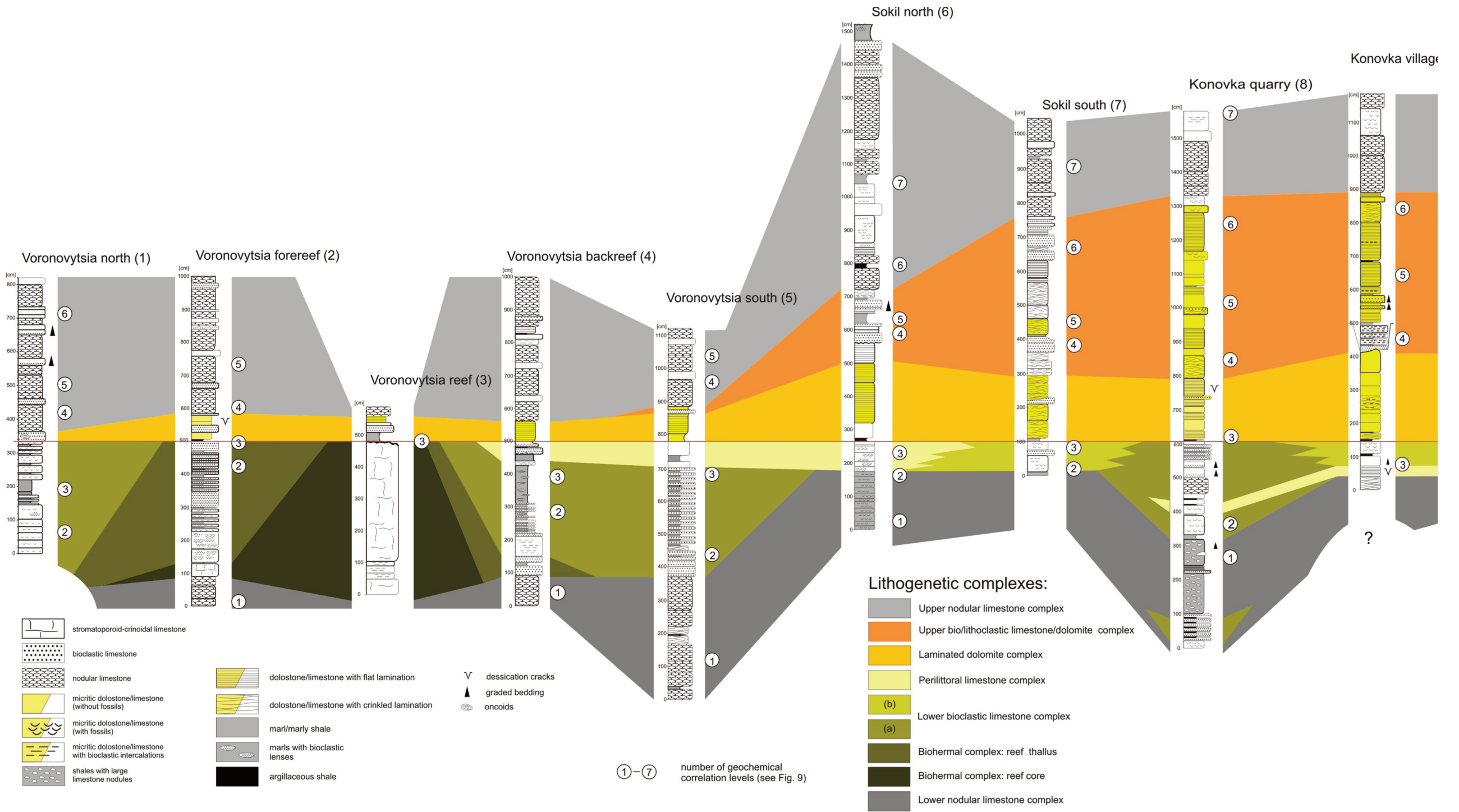
The lower part of the succession embraces deposits representing a shallowing-upward trend. The sedimentary environment, initially uniform bathymetrically, became much more diversified in the later stages. In the final stage, local emersions took place, which resulted in the occurrence of stratigraphic gaps in some of the sections.

#### *Lower nodular limestone complex*

**DESCRIPTION:** The lowest facies in most of the sections above the water level of the Dnister is a monotonous complex of lower nodular limestones (Text-fig. 4). The more or less individualized nodules are embedded in a marly matrix (Text-fig. 5A, B), with varying proportions of the two components. The spectrum ranges between a few up to a dozen or so centimetres thick limestone layers interbedded with centimetre-thick dark grey or greenish clays, at one end, and marly layers with loosely scattered nodules of pure limestones, at the other. The nodular limestones contain an abundant fauna of various leperditid ostracods, small stromatoporoids and tabulate corals (with dimensions not exceeding a few centimetres), common gastropods and rare nautiloids. The marly intercalations abound in small brachiopods belonging to the *Camarotoechia* assemblage (*sensu* Gritsenko *et al.* 1999). Microfacially, the limestones are represented by bioclastic wackestones and occasional brachiopod packstones, with common bioturbations. A character-



Text-fig. 3. General view of the section on the Dnister riverside near Voronovytsia village. A – Central part of the section with a bioherm arrowed in black (section no. 3, enlarged on Fig. 3B); boundary between Shutnivtsi and Sokil "Members" is indicated by a white arrow. B – Transition of the coral-stromatoporoid-crinoid bioherm into a thin-layered backreef complex. C – Tabulates, overturned stromatoporoids, broken crinoid stems and carbonate nodules in the transitional layers (reef core/proximal thallus)



Text-fig. 4. Correlation and facies scheme of the sections studied

istic feature differentiating the nodular limestones of the lower part of the succession from those occurring higher in the sections, is a relatively low content of crinoids, which are restricted to the thin intercalations.

The complex of lower nodular limestones embraces also micritic limestones with fossils. Microfacially these are loosely packed wackestones with well-preserved faunas. From typical nodular limestones, they differ in terms of a greater lateral continuity of particular beds and in a lower proportion of clay-marly intercalations. In some cases, the micritic limestones show subtle horizontal laminae, or contain grained intercalations, occasionally with normal grading. The fossil content is typical of the nodular limestones, only enriched by sporadic occurrences of dendroid rugose corals.

**INTERPRETATION:** The lower nodular limestones represent a typical shelf deposition in a subtidal zone (Nikiforova and Predtechensky 1968; Predtechensky *et al.* 1983; Skompski *et al.* 2006; Racki *et al.* 2012). A low-diversity brachiopod association (resembling that reported from the Tofta Beds on Gotland, ascribed by Watkins (1992) to Silurian back-reef settings), the common occurrence of leperditid ostracods (see Vanier *et al.* 2001), the abundance of gastropods and the dark colour of the sediments, all suggest some isolation of the sedimentary environment, with a rich input of clay material. Simultaneously, a lack of rich crinoid accumulations, and a generally low content of rugose corals with, simultaneously, a large quantity of tabulates and with a high clay content, indicate that the sediments formed in an internal shelf zone (*sensu* Einasto *et al.* 1986) that was separated from outer shelf by areas dominated by stromatoporoids forming biostromes, parabiostromes and (less commonly) bioherms. The nodular limestones most probably represent the deepest facies of the lower part of the succession.

#### *Biohermal complex*

**DESCRIPTION:** The complex encompasses the biohermal facies and the accompanying thallus facies, and is distinctly discernible from the surrounding sediments. Unfortunately, it is hardly accessible, and its features could be traced only in three sections (Voronovytsia forereef (2), Voronovytsia reef (3) and Voronovytsia backreef (4)). In the central section – Voronovytsia reef (3), the complex is developed as massive, unbedded biogenic limestones (Text-fig. 3A, B) rich in stromatoporoids, rugose corals, tabulates, crinoids and brachiopods. Particular parts of the car-

bonate buildup are separated by clay intercalations. The abundant crinoids occur as individual ossicles and non-separated stems, and reach a particularly large diameter of up to over 2 cm. The crinoid content increases upwards. The complex upper boundary is distinctly erosional. The lower part of the complex is more marly and is developed as marly limestones with flasers of bioclastic material. This part contains abundant tabulates and rugose corals accompanied by crinoids and rare brachiopods. The thallus facies are developed as bioclastic limestones and pelitic limestones with bioclasts (Text-fig. 3C); usually thin-bedded, but in places forming thicker beds (Voronovytsia forereef (2) section). Microfacially the bioclastic thallus facies are represented by coarse-grained packstones with large fragments of tabulates, stromatoporoids and scarce rugose corals. Their most conspicuous and common components are large crinoid ossicles. In the pelitic limestones, microfacially dominated by densely packed crinoidal packstones, the bioclastic content is the same but the crinoids usually occur as long stems, and are sporadically accompanied by nautiloids. The microscopic picture reveals the occurrence of common bryozoans, rare fragments of trilobites and tentaculitids, as well as echinoid spines.

**INTERPRETATION:** The massive lithology and the abundance of the typical biotic components allow the complex to be interpreted as a stromatoporoid-coral-crinoid buildup. The lack of specific cements hinders a more detailed classification. The bottom of the bioherm is submerged beneath the Dniester (Text-fig. 3A, B), however the analysis of adjacent sections indicates that the observations of its accessible part embrace most of its height. The same is confirmed also by the limited extend of the thallus facies. However, it seems probable that in the direction perpendicular to the wall's exposure, the bioherm extends for a much larger distance. This can be inferred from the role that the bioherm has played in governing the distribution of sedimentary environments throughout the section. The distinct difference of sedimentary development throughout the sections on the fore- and back-sides of the bioherm suggests that it constituted a long and important barrier, or was part of a belt of isolated buildups, which formed a barrier zone.

#### *Lower bioclastic limestone complex*

**DESCRIPTION:** This complex, which formed during intervals characterized by a diversified morphology of the sea bottom, embraces two main lithotypes. The first type (a) is represented by rhythmically deposited





bioclastic deposits (fine and medium-grained calcarenites) with clay, marly or pelitic intercalations. The thickness of the bioclastic beds ranges between a few and a dozen or so centimetres. In some parts, the bioclastic beds are discontinuous and form elongated lens-shaped bodies (Voronovytsia backreef (4) section). Some of the beds show normal grading. The thickness of the clay-marly intercalations usually does not exceed 10 cm. The pelitic beds often show horizontal laminae. The whole complex is characterized by a rich fauna, which, however, can be identified in detail only in its marly parts. The calcarenites are represented by bioclastic packstones dominated by crinoids and shelly fossils (Text-fig. 6A). Also sporadically present are larger clasts of stromatoporoids, tabulates and rugose corals (Text-fig. 5B). The main biotic components of the clay-marly intercalations are brachiopods of the *Chonetes* and *Camarotoechia* assemblages (*sensu* Gritsenko *et al.* 1999) and some of the intercalations show the character of brachiopod shell-beds (coquinas). The complex contains abundant crinoids, usually preserved as individual ossicles, less commonly by short non-separated stems. Fragmented tabulates (*Favosites*), massive and branching (*Amphipora*) stromatoporoids and rugose corals are the most common accessory components. The rhythmical succession is sporadically obscured by the occurrence of large clasts derived from reefal structures – mainly stromatoporoids and tabulates.

In part of the sections (e.g. Konovka quarry (8)), the rhythmically deposited bioclastic limestones are also partly developed as nodular limestones. A feature that distinguishes them from the typical nodular limestones of the lower complex is the rich occurrence of crinoids, which are absent from the lower sections. Another variety of rhythmites is represented by thin beds of marly shales with lenses of bioclastic material derived from the destruction of reef buildups.

The second lithotype (b) is best exposed in the lower part of the Sokil south (7) section. It is represented by pelitic limestones with concentrations of ostracods and brachiopods and with rare overturned and broken individual stromatoporoids and tabulates. The bottom parts of the beds yield rounded clasts of micritic limestones. The whole complex abounds in bioturbation structures, some of which can be recognized as individual burrows of animals penetrating the sedi-

ment. Wavy beds of biogenic origin are a typical feature throughout the whole complex. Also relatively common are oncoids, which reach a diameter of up to 2 cm (Text-fig. 6B). Their coatings with well-preserved microorganisms (Text-fig. 6C, D) contain girvanellid-sphaerocodial green algae (genus *Garwoodia?*) and cyanobacterial layers. According to the observations of Einasto and Radionova (1988) such type of oncoids usually formed in the direct vicinity of stromatoporoid bioherms, on their back-barrier side. At a greater distance from the barriers, in central parts of the lagoons, oncoids formed with purely spongiostromid coatings, which are distinctly different from those found in the sections described. The same type of oncoids has been described by Łuczyński *et al.* (2009) from the Zubrivka section on the Smotrych riverbank, and has been interpreted as formed in a back-barrier, but relatively high-energy setting, as indicated by their generally spherical shapes. Usually their occurrence preceded the onset of biolaminitic facies – as is the case also in the analysed sections.

**INTERPRETATION:** Both lithotypes of the lower bioclastic limestones complex formed during a stage characterized by variable sea bottom morphology. The shallower zones acted as alimentation areas for the bioclastic material, which was deposited in local depressions on the shelf. The redeposited material contained elements of a diverse biocenosis characteristic of a shallow water, well oxidized environment, dominated by populations of rugose corals, tabulates, stromatoporoids and crinoids. The host material of the depressions is represented by clay-marly sediments with a rich brachiopod biocenosis. The analysis of the whole lower part of the succession points out that shallow water zones developed around biohermal buildups, which probably suffered occasional emersion and subaerial erosion and acted as source areas for large clasts of reef-type material. Away from the shallow zones, the sediments had the character of marly limestones, which in early stages of diagenesis often altered into nodular limestones, but with a distinct admixture of crinoid material. Gradual infilling of the depressions led to the occurrence of lithotype (b), with a noticeably lower amount of bioclastic material, and to the onset of shallow water sedimentation of biogenic laminites and oncolites.

Text-fig. 5. Sedimentary features of the described complexes. A, B – Lower nodular limestone complex; intercalations of micritic and bioclastic limestones within grey argillaceous shales, note a single stromatoporoid dome in growth position, surrounded by shales; Konovka village (9) section. C – Bioclastic limestone with broken stromatoporoids, corals and ostracods; note erosional boundaries of the layer; Sokil south (7) section, lower part of upper bio/lithoclastic limestone/dolomite complex. D – Contact of dolomitic laminites with bioclastic calcarenite, note stromatoporoid dome, covered by grained material: Sokil north (6) section, bottom part of the upper bio/lithoclastic limestone/dolomite complex. E, F – Microbial, dolomitized laminites, with some laminae ripped by tidal (?) currents (F); Konovka village (9) section, laminated dolomite complex. G – Bioclastic rudstone, dominated by stromatoporoid clasts; upper bio/lithoclastic limestone/dolomite complex, Sokil north (6) section. H – Hummocky cross-stratification in the laminated dolomite complex, Konovka village (9) section

*Perilittoral limestone complex*

**DESCRIPTION:** This complex is lithologically diverse; however, some of its features point to a distinct shallowing of the sedimentary environments as compared to the complexes described above. The complex reaches a thickness up to 1 metre and is usually composed of thin beds of pelitic limestones (grained in places) accompanied by a dozen or so centimetres thick layer of black, greenish or yellowish clays. The biotic components represent an impoverished assemblage usually restricted to leperditid ostracods. In the case of bioclastic intercalations (lenses) the biogenic content is slightly enriched by stenohaline components, such as rugose corals and tabulates. Microfacially the limestones are represented by peloidal-shell wackestones, most commonly with ostracods. Bio-laminations and bioturbations are common and are accompanied by fenestral structures. In the most conspicuous case (Konovka village (9) section), the laminitic limestones contain desiccation cracks.

**INTERPRETATION:** The described complex can be attributed to an episode of maximum shallowing, during which carbonate sedimentation persisted only in small local basins, probably with anomalous salinity resulting in an impoverishment of the biotic assemblage. In the biohermal zones, the interval is hidden in a postulated stratigraphic gap, corresponding to sub-aerial erosion of the stromatoporoid buildups. As expected, the complex is best developed in the most proximal zone, represented by the Konovka village (9) section. In the more distal zones (Voronovytsia north (1) section), the shallowing interval found no distinct expression in the stratigraphical succession. A regressive shifting of the carbonate production zones towards open sea areas resulted in the occurrence of distinct clay layers, the colour of which was governed by local sources of organic material.

**Upper part of the succession**

The upper part of the succession is composed of three complexes with varying thickness and distribution. In stratigraphical order these are: laminated

dolomite complex, upper bio/lithoclastic limestone/dolomite complex and the upper nodular limestone complex.

*Laminated dolomite complex*

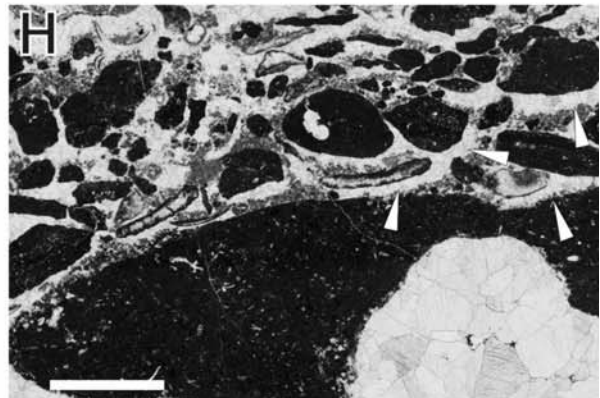
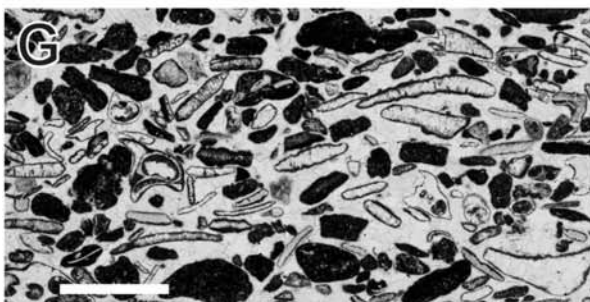
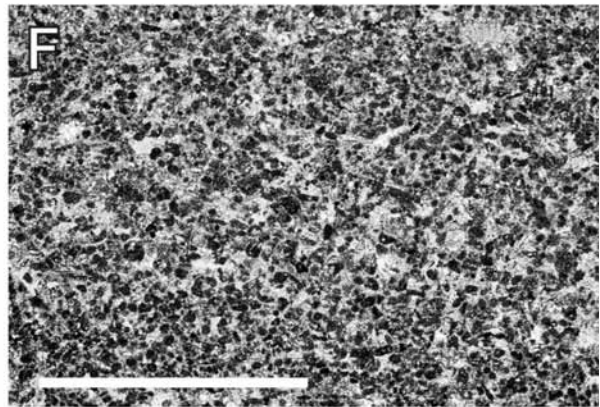
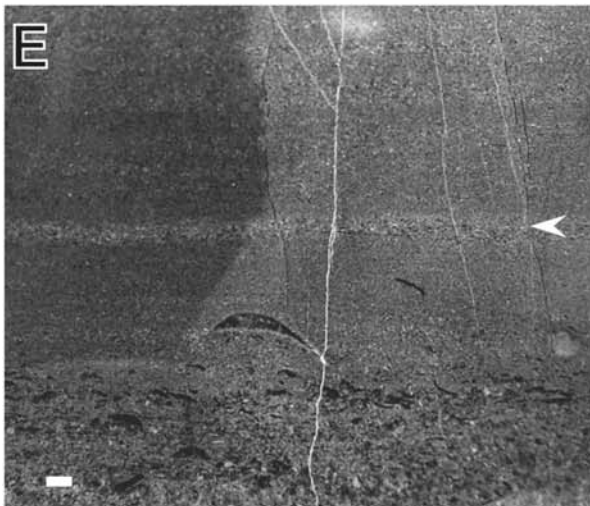
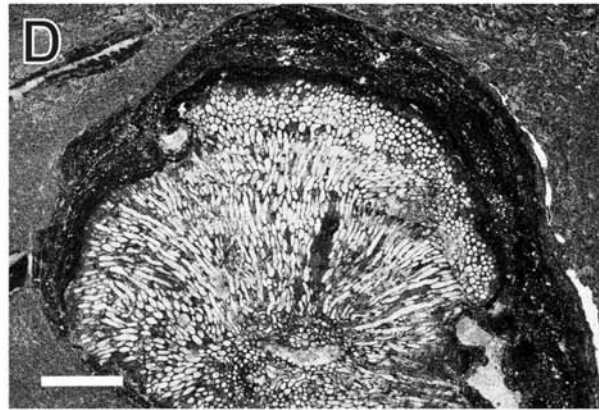
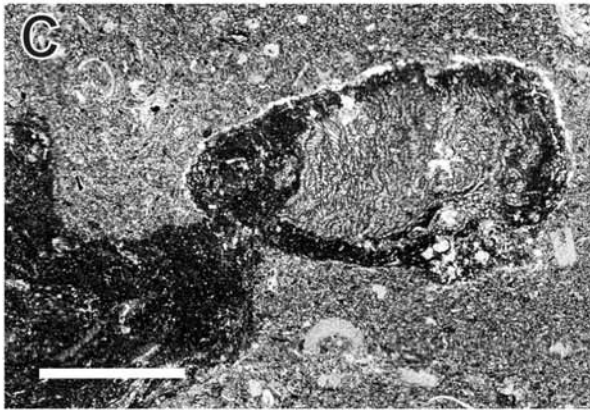
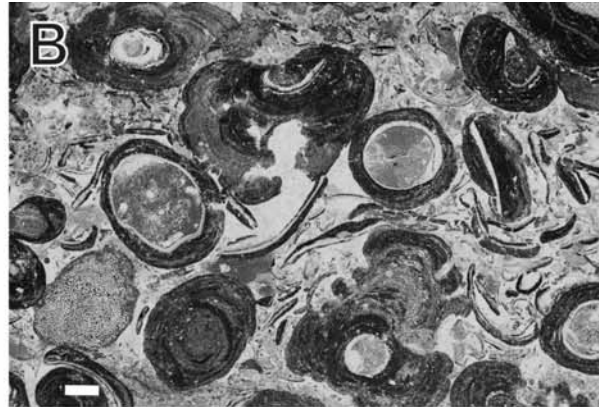
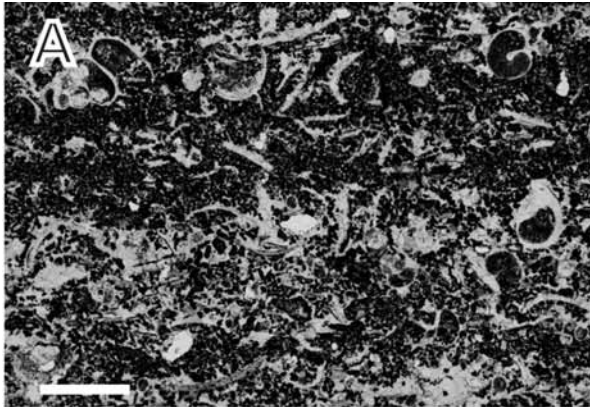
**DESCRIPTION:** This complex embraces an interval with a thickness of up to 2–3 metres, characterized by the occurrence of pelitic dolomites, with wavy beds, if the laminae are of biogenic origin, or with horizontal beds, if it is an effect of intercalating thin pelitic and grained laminae (mechanical laminae). Its thickness, relatively small in the northern part of the study area, increases distinctly southwards to reach its maximum near the village of Konovka (9). In most of the sections, the complex is marked by the occurrence of dolomites and a general scarcity of fossils; however geographically it shows a conspicuous internal variability, e.g. in the Sokil north (6) section it starts with micritic limestones with ostracods.

In the northern part of the study area (sections Voronovytsia forereef (2), Voronovytsia reef (3), Voronovytsia backreef (4) and Voronovytsia south (5)), the complex with its thickness not exceeding 1 metre, is represented by horizontally bedded dolomites with grained interlayers and inclusions, and with thin limestone intercalations. The fossil content in the dolomites is limited to ostracods, while the limestone beds also contain brachiopods, crinoid ossicles and small (up to 1 cm) stromatoporoid fragments. The complex is also characterized by the occurrence of small oncoids and micritic lithoclasts, which often show imbrications. Desiccation cracks occur locally.

In the northernmost section – Voronovytsia north (1), the equivalent of the dolomitic complex is represented by a calcarenitic bed rich in fossils (stromatoporoids, tabulates, gastropods, and shell debris) and with oncoids and micritic lithoclasts.

In the southern part of the study area (sections Sokil north (6), Sokil south (7), Konovka quarry (8) and Konovka village (9)), the complex reaches a thickness of 2–3 metres, and reveals a more conspicuous lithological variability. In the Sokil region, the dolomites show distinct wavy (more often) and horizontal laminae (Text-fig. 7A, B). Commonly, how-

Text-fig. 6. Specific microfacies of limestone complexes. Length of scale = 2 mm. A – Peloidal-bioclastic packstone, with components dominated by gastropods and oncoids; Konovka village (9) section; the lower bioclastic limestone complex. B – Oncolitic rudstone; Sokil south (7) section, bottom part of the lower bioclastic limestone complex. C – Girvanellid-sphaerocodial oncoids; Sokil south (7) section, bottom part of the lower bioclastic limestone complex. D – Microbial coat developed on the cyanobacterial (*Garwoodia* ?) core; Sokil south (7) section; bottom part of the lower bioclastic limestone complex. E – Graded calcarenites to calcisiltites from intercalations within the upper nodular limestone complex; lamina with admixture of dolomite grains indicated by an arrow; Voronovytsia north (1) section. F – Peloidal packstone; typical microfacies of calcisiltitic intercalations within upper part of the upper nodular limestone complex; Voronovytsia north section (1). G – Bioclastic grainstone dominated by crinoid, gastropod and molluscs debris; Sokil south (5) section; bioclastic lens within the upper bio/lithoclastic limestone/dolomite complex. H – Litho-bioclastic grainstone with pendant cements (white arrows); Konovka village (9) section, infilling of the erosional channel in bottom part of the upper bio/lithoclastic limestone/dolomite complex



ever, the laminae are dynamically ripped and the beds are effectively developed as a breccia composed of long, horizontally laminated intraclasts derived from the underlying sediments. The laminites often contain large bioclasts of bulbous and tabular stromatoporoids, tabulates and rugose corals, which have been thrown into an environment of sediments deposited in calm conditions (Text-fig. 7A, B). Numerous oncoids and thin layers with abundant ostracods are also common. The relatively rare grained intercalations with coarse-grained material reveal normal grading and a tempestitic (convex up) arrangement of the bivalve shells. The fine-grained beds contain hummocky cross-stratifications (Text-fig. 5H). The upper boundary of the complex is distinctly erosional. In the southernmost region of Konovka the sedimentation of the laminites took place in distinctly calmer conditions. The layers are less commonly ripped, and subtle wavy laminae prevail (Text-fig. 5E, F). The grained intercalations are replaced by pelitic layers, with only faint trails of bio/lithoclastic material. A periodic increase of sedimentation dynamics is inferred only by the occurrence of thin layers of flat pebble conglomerates with relatively small pebbles. Fossils and oncoids are practically absent.

**INTERPRETATION:** The described dolomitic complex is a textbook example of an initial phase of a transgression on a carbonate shelf. A vast shallow-water platform, probably dominated by peritidal environments, was a place of sedimentation of carbonate sediments, which were subjected to very early dolomitization (eogenetic dolomites). Such an origin of the dolomites is indicated by their general micritic character and by the perfect preservation of the sedimentary structures (laminae, desiccation cracks, fenestral structures, etc.). The lack of accompanying evaporites, or of their traces, allows exclusion of the sabkha model, and indicates instead dolomitization under the conditions described in the Dorag model. Temporary flooding of the whole tidal flat area by marine waters during storms, as indicated by tempestitic structures, was the main factor enabling early dolomitization. The spatial variability of the complex development reflects the palaeogeographic situation inherited after previous stages of deposition. In the northern part of the area, the occurrence of limestone intercalations points to a contact with open marine environments. Southwards the open marine influence decreases (as does the contribution of material derived by storms), which makes it indiscernible in the Konovka region. The most dynamic changes in the sedimentary environment took place in an area corresponding earlier to the Voronovytsia biohermal struc-

ture (Sokil area). The laminites deposited in calm conditions were destroyed here during high-dynamic episodes, most probably by storms. The region probably functioned as a shallow-water shoal that acted as a barrier, separating the northern zone contacting with open marine environments from the restricted lagoonal zone of Konovka.

The dolomitic complex has numerous counterparts described in the sedimentological literature (e.g., Ward and Halley 1985; Ruppel and Cander 1988; Meyers *et al.* 1997; Davies and Smith 2006; Kiipli and Kiipli 2006). A complex of eogenetic dolomites at the beginning of the development of the Devonian carbonate platform of the Holy Cross Mountains in central Poland (Racki 1993; Narkiewicz 1988, 1990) is one good example of such sedimentary conditions.

#### *Upper bio/lithoclastic limestone/dolomite complex*

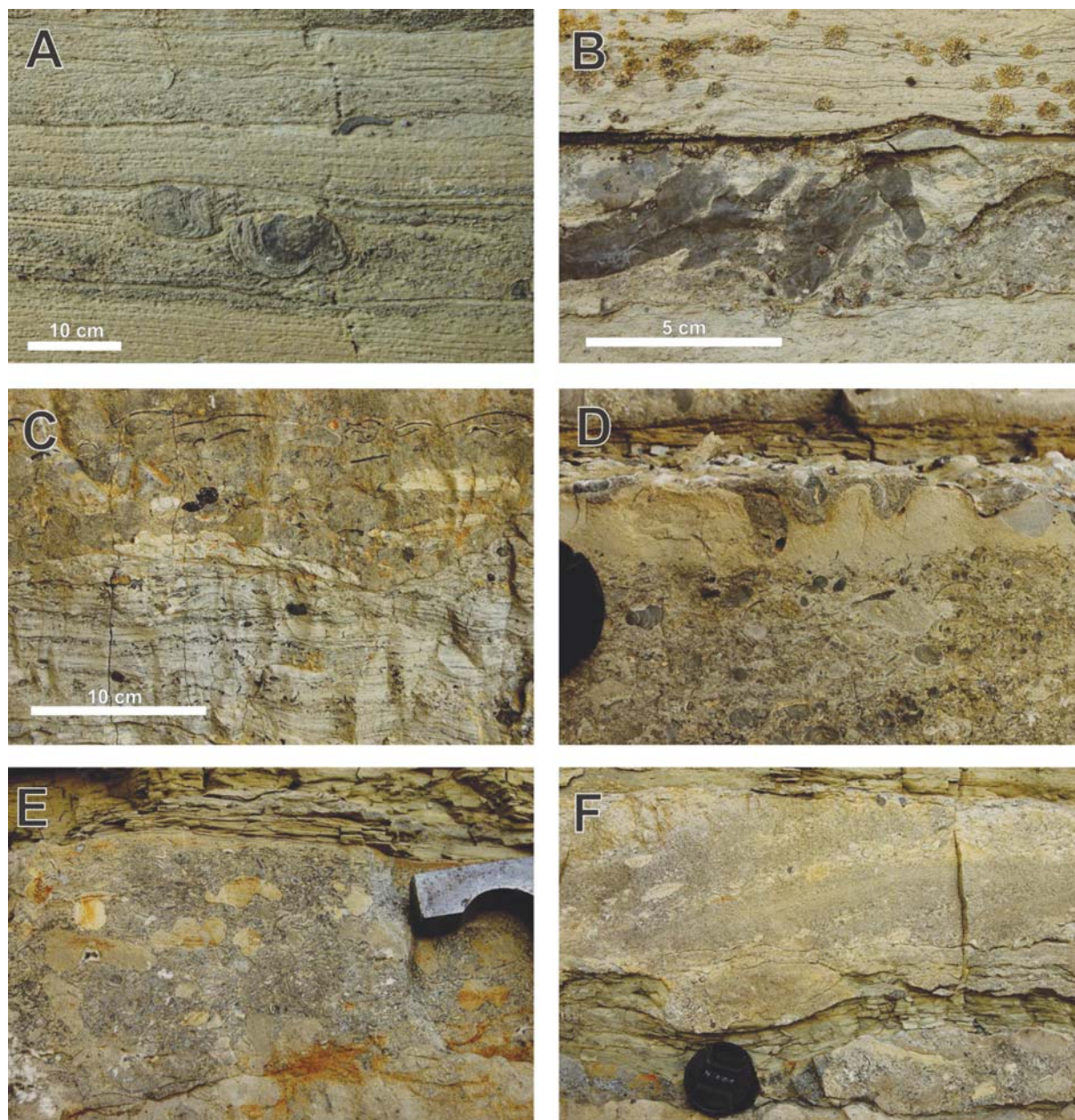
**DESCRIPTION:** This complex is exposed only in the southern part of the study area, in the Sokil and Konovka regions. Its development largely corresponds to the underlying complex of laminated dolomites but with a conspicuously higher share of the purely calcareous bioclastic and lithoclastic facies.

In the Sokil region, the complex is composed mainly of bio/lithoclastic limestones, commonly forming beds several tens of centimetres thick (an extraordinary feature throughout the entire study area). Usually the beds are developed as coarse-grained calcarenites (Text-figs 5G, and 7A–F) full of debris of stromatoporoids (with diameters of up to 10 cm), tabulates, rugose corals, bivalves, ostracods and oncoids (Text-fig. 5C, D), in some places showing cross bedding (Text-fig. 7F). The numerous intraclasts are commonly derived from distinctly bioturbated limestones, and some of the micritic clasts show “plastic” outlines, indicating that the disintegrated rocks were partly unconsolidated (Text-fig. 7E). Some of fine-grained intercalations show normal grading. Microfacially the bio/lithoclastic limestones are represented by intraclast-crinoidal grainstones and rudstones (Text-fig. 6G) with detritus of bryozoans, tabulates, rugose corals, stromatoporoids, ostracods and oncoids. The complex contains rare laminated deposits (with both horizontal and wavy beds), as well as flat pebble conglomerates with clasts derived from their destruction. The laminitic beds are often dolomitized.

In the Konovka region, this part of the succession is strongly dolomitized and the limestones occur only subordinately. The most conspicuous occurrence of limestones is that of an infilling of an erosional channel exposed in the Konovka village (9) section. A metre-

deep structure is filled by intraclast-bioclastic limestones with ostracods, nautiloids, rugose corals, tabulates, gastropods and stromatoporoid fragments (Text-fig. 6H). The surrounding dolomites are developed as laminites with both horizontal and wavy laminae, and contain relatively common beds with flat pebble conglomerates. The laminites are accompanied by thin-bedded micritic dolomites, devoid of fossils. Occasional graded intercalations reveal normal grading.

INTERPRETATION: The sedimentological interpretation of this complex is radically different from that of the above-described complex of laminated dolomites. Admittedly, the deposits exposed in the Konovka region are typical of tidal flats and embrace biogenic and mechanical laminae, but evidently more frequent are sediments deposited in high-dynamic conditions. The flat pebble conglomerates have been formed during washing away of consolidated and semi-consolidated



Text-fig. 7. Sedimentary features of the upper bio/lithoclastic limestone/dolomite complex. A, B – Overturned and broken stromatoporoids within biocalcirudites, intercalated with laminites; Sokil north (6) section, bottom part of the upper bio/lithoclastic limestone/dolomite complex. C – Contact of biolaminites with a tempestitic layer with ripped laminae, broken stromatoporoids and tabulates, leperditids, lithoclasts and bivalves with convex up arrangements of shells; Sokil north (6) section, bottom part of the upper bio/lithoclastic limestone/dolomite complex. D, E, F – High-dynamic calcirudites with bioclastic and lithoclastic components; note erosional boundary of the layer (D), coated, plastic lithoclasts (E) and large-scale cross-laminae (F); Sokil north (6) section, bottom part of the upper bio/lithoclastic limestone/dolomite complex

bottom sediments in tidal conditions, and backwash channels have been filled with material derived by on-shore transport (compare, Skompski *et al.* 2008; Łuczyński *et al.* 2014). In the Sokil area, the dolomitic succession is replaced by extremely high-dynamic limestone facies, with numerous erosional surfaces (Text-figs 5C, D and 7D), which indicates the influence of open-marine environments.

#### *Upper nodular limestone complex*

**DESCRIPTION:** This complex is a close counterpart of the above-described lower nodular limestones; however, it includes a number of thin specific layers, composed of very fine-grained or “pelitic” deposits. Some of them indicate normal grading. In the northern part of the area, these beds can be treated as correlation horizons. Microfacially the aforementioned beds are represented by monotonous peloidal packstones (Text-fig. 6F) with large individual bioclasts (e.g. of gastropods), or by bioclastic packstones/wackestones, in some cases bioturbated or featured by evident normal grading (Text-fig. 6E).

**INTERPRETATION:** Although, from a purely descriptive point of view, the main components are classified as peloids, genetically they correspond to the “small intraclasts” of Wilson (1967), or to the “pseudopellets” of Fahraeus *et al.* (1974) that formed during erosion of a weakly lithified carbonate mud. Their size, sorting and spectrum of shapes, as well as mixing with fine-grained fossil debris, allow these grains to be classified as “mud peloids” or “lithic peloids” *sensu* Flügel (2004, p. 113). The allochthonous nature of these grains is also emphasized by the presence of numerous silt-sized dolomitic particles in the matrix (Text-fig. 6E). This can be treated as an important argument pointing for an origin of the “pelitic” beds as an effect of washing out of fine clastic material from the edge of a shallow water carbonate platform, which developed southward of the study region.

The nodular limestone complex represents the deepest sedimentary environment recorded in the analysed sections.

#### CORRELATION LEVELS REVEALED BY GAMMA RAY MEASUREMENTS

The seven correlation levels (Text-fig. 8) defined below were selected for the most evident sequence stratigraphic events, which, however, were often fully discernible only in single sections. The spectral

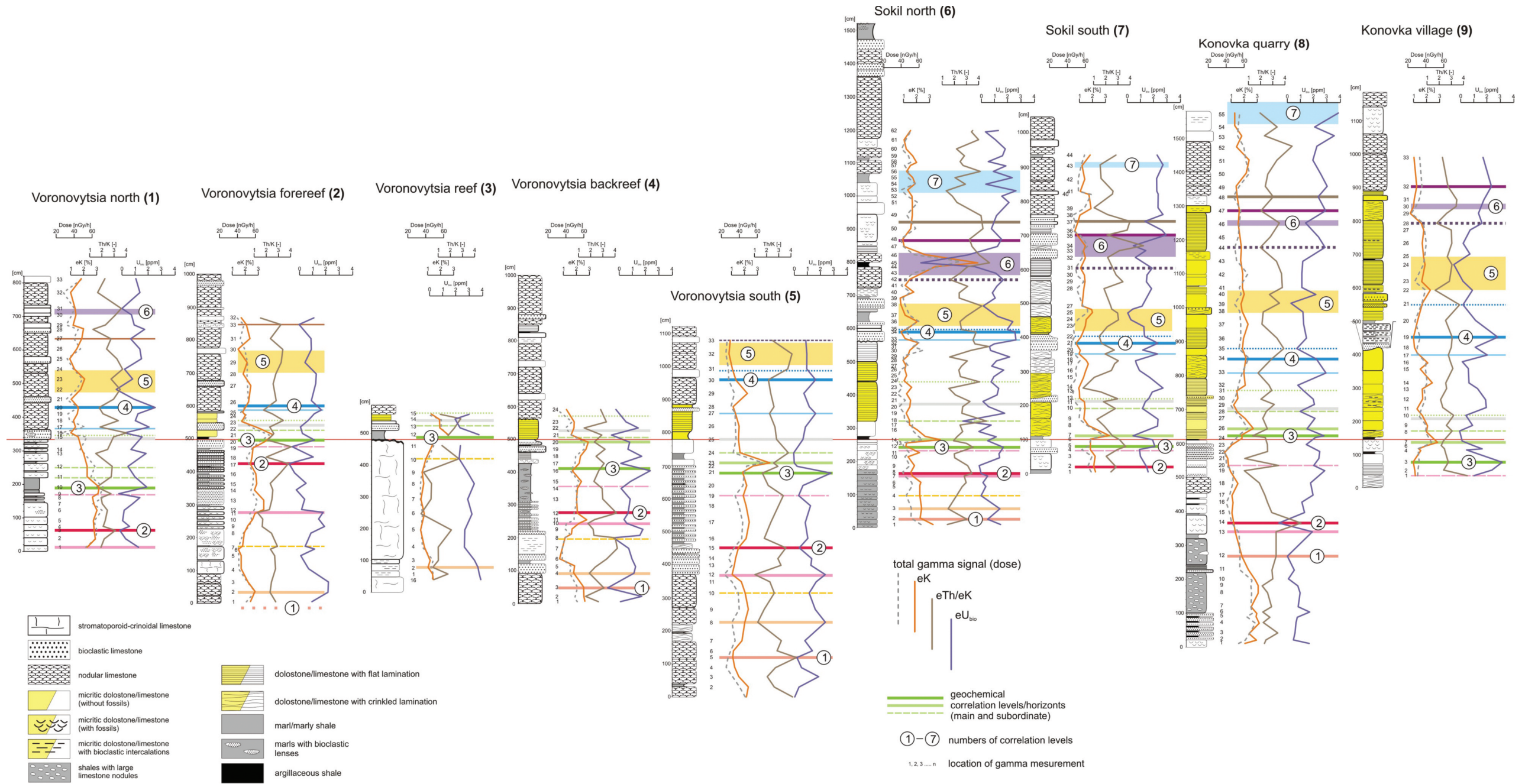
gamma ray (SGR) data were used for lateral tracking of easily interpretable sedimentary events and for discovering their less evident counterparts. Less distinct subhorizons are also indicated on figure 8 by coloured and dotted lines.

**Horizon (1)** is defined by a distinct positive Th/K peak coinciding with low  $U_{\text{bio}}$  values. The level can be tracked laterally within the lower nodular limestones in sections 2, 4, 5, 6, and 8. In sections 2–4, the horizon roughly corresponds to the base of a 5 m thick stromatoporoid-coral-crinoidal bioherm (“Voronovytsia Reef”) surrounded by auto-thallus facies, which is embedded within the uppermost part of the lower nodular limestones. Locally, probably on minor elevations (sections 5 and 8), the level is marked also by initial bottom colonization by tabulate corals.

**Horizon (2)** is defined by an initial increase of the Th/K ratio paralleled with low  $U_{\text{bio}}$  values. It is also recorded by the start of an increase in potassium content. Its reflection in facies development is variable. In section 3, the top of the Voronovytsia Reef is cut by an erosional surface, with a gap including (also after physical correlation) horizons (2) and (3). In the fore reef section (section 2), the relief infilling succession starts with pseudo-thallus facies composed of reef-derived clasts (up to 30 cm in diameter). In other sections, the horizon is marked by deposition of limestones with re-deposited faunas (sections 4, 5 and 8) and by sea-bottom colonization (sections 6 and 7). North of the Voronovytsia Reef area, the event is recorded by fore stepping of a patch-reef system, with development of small reefs in the former fore-reef area.

**Horizon (3)** is defined by a distinct peak in  $U_{\text{bio}}$  values, coincident with a high Th/K ratio and maximum potassium abundances. In sections 6 and 7, the event is marked by the appearance of a 10 cm thick black shale layer, interpreted as formed during a sediment starvation episode due to emersion of the platform top, and by changes in the ecosystem recognizable in the biofacial record. In distal sections (section 1) the horizon is developed as a characteristic individual marl bed, formed due to a break of carbonate production on the platform top. Similar clay-rich sediments fill local depressions in some other sections (sections 4, 5 and 8), passing laterally into more marginal marine facies. In section 9, the level is marked by the occurrence of surfaces with desiccation cracks.

The peak of  $U_{\text{bio}}$  values that defines horizon (3) is followed by a negative shift that can be laterally tracked throughout the sections. The erosional top of



Text-fig 8. Spectral gamma-ray correlations of the sections studied



the Voronovtsia Reef (section 3) is capped by a 1 m thick succession dominated by marls and laminated dolomites. Facially, the interval is recorded by facies unification, with common sedimentation of laminated dolomites protruding into distal zones (section 2). In the most distal setting (section 1), the level is developed as brachiopod coquinas and grainstones.

**Horizon (4)** is defined by a distinct peak in the  $U_{\text{bio}}$  content. Inside the dolomite platform the event is recorded by infilling of a tidal channel by limestones with open marine faunas (section 9), and can be tracked laterally within the mechanical laminites of the upper bio/lithoclastic limestone/dolomite complex (sections 7, 8). In section 6, the level marks the end of sedimentation of platform laminites, indicating a retrogradational facies array. In distal areas (sections 1–5), the horizon is manifested by the occurrence of the first of a suite of characteristic calcilutite marker beds.

**Horizon (5)** is manifested by a thick interval of low  $U_{\text{bio}}$  values following the peak defining horizon (4). Facially it is represented by an expansion of the carbonate platform deposits and by a retrogradational facies array and by the occurrence in distal sections of characteristic calcilutites, which formed due to the export of large amounts of carbonate material from platform interiors during stronger high-energy events.

**Horizon (6)** is defined by low  $U_{\text{bio}}$  values coincident with a peak in the Th/K ratio. It follows an interval with high  $U_{\text{bio}}$  values paralleled with gradual increase of the Th/K ratio, which in the facies record is manifested by the end of dolomite platform sedimentation in proximal sections (6–9), and by deposition of transgressive nodular limestones. In the most distal section (1), the horizon is marked by a calcilutite bed.

In section 6, the first bed of nodular limestones is capped by a 20 cm thick layer of greenish clayey shales with extreme potassium concentration and with the maximum noted Th/K ratio. This clay layer is interpreted as bentonite M1 by Tsegelnjuk (1974, fig. 27) and Tsegelnjuk *et al.* (1983, fig. 9). Most probably the same level is recorded also by Środoń *et al.* (2013) and Huff *et al.* (2000, fig. 4). In the latter work, it is marked also in the section of Konovka. However, in our sections, the shale layer does not occur south of Sokil (probably due to erosion in extremely shallow water facies); nonetheless, its time equivalent can be traced as our correlation level (6). Similarly, in the northern sections, the shale (bentonite) layer is absent, but its equivalent is identified as level (6) in the Voronovtsia north (1) section.

**Horizon (7)** can be traced only in sections 6–8. It is marked by rapid fluctuations of  $U_{\text{bio}}$  values, however maintaining their high levels. Sedimentation of nodular limestones prevailed throughout the area. Higher in the distal sections (1, 2), the nodular limestones are intercalated by thin layers of pelitic limestones (in hardly accessible parts of the exposures not illustrated on figs 3 and 4), which indicates that the sedimentation took place from suspended fine carbonate material.

It is worth emphasizing that most SGR correlation horizons, and particularly horizons (4), (5) and (6), appeared here independently of facies, and played an original role in the identification of time levels. An important role in correlating the sections was played also by thin layers of pelitic/peloidal limestones (calcilutites), which are particularly evident and could be tracked between the sections in the offshore area of sedimentation.

## FACIES DEVELOPMENT

The general transect composed of the sections exposed along the Dnister River between the villages of Voronovtsia and Konovka stretches roughly NW–SE (Text-fig. 1C). The emerging facies array points to its more or less perpendicular orientation in relation to the hypothetical shoreline, which is very convenient for facies interpretations. The applied chronostratigraphic framework is based on gamma ray correlation, which allowed drawing a number of lines, most of which enable defining the architecture of lithofacies units more accurately.

The studied stratigraphic interval can be divided into six main development stages, with the first three representing a regressive stage and the last three a transgressive stage of the basin's history (Text-fig. 9):

- phase I – unified sedimentation on a deep sea bottom;
- phase II – development of the bioherm and its accompanying facies;
- phase III – shallowing of sedimentation and erosion of the bioherm;
- phase IV – first transgressive impulse, initiation of a new carbonate platform;
- phase V – retrogradational shifting of shallow water facies with lithofacies record of the re-flooding-window
- phase VI – unified sedimentation on a deep sea bottom

*Phase I* represents the time of unified sedimentation of shelf marly deposits that during early diagenesis

altered into nodular limestones. The taxonomic composition of the faunal assemblages, combined with the dark colours of the sediments, suggest an isolated sedimentary area richly supplied with clay material. The limestones probably formed in the inner part of the shelf (*sensu* Einasto *et al.* 1986), separated from the open marine zones by a belt dominated by stromatoporoids forming numerous biostromes, parabiosomes and (relatively rare) bioherms. The nodular limestones represent the deepest facies of the lower part of the succession, deposited during initial still-stand conditions (HST). Correlation horizon (1), identified in the uppermost part of the nodular limestone complex, represents an initial sea level fall of the late HST and marks the onset of the formation of the Voronovytsia Reef.

*Phase II* started with a conspicuous lowering of the sea level and differentiation of the sea bottom morphology. The differentiation was caused by the growth of small stromatoporoid-coral-crinoidal bioherms, such as the one recognized in the Voronovytsia reef (3) section. Sedimentation of bioclastic limestones with clay-pelitic intercalations and pelitic limestones with bioclasts took place in the areas between the bioherms.

Correlation horizon (2), marking the onset of the Voronovytsia Reef emersion, represents the beginning of a forced regression. In SGR parameters, the potassium content increase is caused by residual clay influx from exposed parts of the platform, and low  $U_{\text{bio}}$  values indicate a higher sedimentation rate.

*Phase III* marks the time of gradual, but substantial lowering of the sea level, the effects of which is distinct in all the sections studied. The top part of the Voronovytsia Reef has been subaerially exposed, and large erosional clasts derived from the reef were transported mainly to the fore-reef basin (Voronovytsia fore-reef (2) section). Both the fore- and the back-reef basins were gradually infilled by deposits, which finally led to local deposition of very shallow facies of the perilittoral limestones complex. On the exposed top of the reef, deposition under subaerial conditions took place for a short period, as indicated by the occurrence of scarce land floral remains (the fossils are currently a subject of palaeobotanical description). *Phase II* and particularly *Phase III* are characterized by the occurrence of a very specific biofacies of large crinoids in both proximal and distal bioherm facies.

Correlation horizon (3), corresponding to the end of *Phase III*, is interpreted as a record of minimum sea level at the end of the LST. The high  $U_{\text{bio}}$  values mark a probable condensation interval or a stratigraphic gap.

Low  $U_{\text{bio}}$  values and facies unification next after horizon (3) indicate accelerated sedimentation and mark the initial flooding, following the end of the LST.

*Phase IV* starts the transgressive stage of the sedimentary development. Shallow waters, in which early dolomitization of the deposited biolaminated sediments took place, covered the whole area, with a unified and flat morphology of the sea bottom. The forming carbonate platform was intensely destroyed during storms, and the laminites were commonly eroded, torn apart and redeposited as flat pebble conglomerates. Areas most vulnerable to destruction of the newly deposited sediments were those adjacent to the bioherms. Only in the northernmost part of the study region, in which the platform contacted with open marine areas, did sedimentation of bioclastic limestones take place.

No SGR horizon is related to this phase, interpreted as the beginning of the TST. It is in agreement with the general features of this facies tract, deposited in a shallow and dynamic environment, usually in the form of isolated sedimentary bodies.

*Phase V* marks the time of a distinct progress of the transgression. The extent of the dolomitic platform became restricted to the southern part of the study area. High-dynamic bio/lithoclastic facies were deposited on the open-marine edge of the platform (Sokil sections). The dynamic facies faded quickly southwards and shallow water laminated or pelitic deposits devoid of fauna, characteristic of calm environments were deposited in the Konovka village region. On the platforms foreland sedimentation of marly deposits took place, which later altered to become the upper nodular limestone complex. Peloidal or bioclastic material was periodically redeposited into the deeper parts of the basin, forming characteristic layers of fine grained or peloidal limestones, which can be treated as local correlation horizons.

The difference in depth between the shallow water dolomitic platform and the basin with nodular limestones was substantial. It can be estimated as at least some dozens of metres. In such a case, platform slope facies should occur but these have not so far been recognized. Such facies should occur between Sokil and Voronovytsia; unfortunately the lack of exposures hinders such observations. Another possible explanation of the lack of observed slope deposits would be an abrupt facies transition, with a very steep slope, as can be suggested by the postulated activity of a fault fringing the platform, the existence of which was evident already in the earlier stages of development.

The interval represented by phase V encompasses correlation horizons (4), (5) and (6). The distinct increase in  $U_{\text{bio}}$  values, defined as horizon (4), indicates slowing down of sedimentation during early phases of transgression, and marks the second flooding surface. The following interval of low  $U_{\text{bio}}$  values (horizon (5)) represents the time of accelerated sedimentation rate caused by the expansion of the carbonate platforms productive area after the flooding event. The next interval of high  $U_{\text{bio}}$  values and gradual Th/K ratio increase is interpreted as the third flooding event. The following horizon (6) with extreme potassium and Th/K values, best evident in section 6, represents the reflooding of the pre-regressive top of the platform, and the export of large amounts of residual clays into the surrounding areas (repayable shale).

The assemblage of levels 4 to 6 is recognizable both within the shallow-water platform facies and within the deeper basin, and thereby this triad gives the most important correlation tool. The recognition of these levels allows the identification of the appearance of the re-flooding window and the confirmation of this by lithofacies observations.

*Phase VI* represents the time of unified sedimentation on a deep-sea bottom. During the increasing sea level, the transgression embraced expanding areas and the nodular limestones facies shifted retrogradationally southwards, capping the dolomite complexes of the shallow water platform. In the final stage basinal nodular limestones formed throughout the area.

High  $U_{\text{bio}}$  values (horizon (7)) mark a distinct condensation horizon connected with maximum flooding. General deepening of sedimentation and an evidently retrogradational facies shift, indicate the initial HST stage of the platform development.

## DISCUSSION

The phases distinguished of the above-described regressive-transgressive cycle have been interpreted in terms of sequence stratigraphy (Text-fig. 9). The study interval is delimited by HST facies (phases I and VI), while its internal part is composed of the late HST (phase II), main and terminal part of the LST (phase III), and finally of the TST and initial HST (phases IV–VI). The details of facies record are generally in agreement with the general models of carbonate sequences (e.g., Hanford and Loucks 1993; Schlager 2005), but at least two lithofacies from the interval corresponding to the transgression, require more detailed comments.

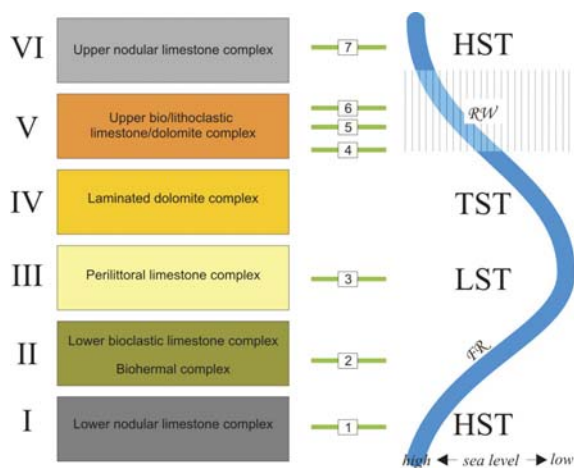
The first lithofacies needing a closer analysis is developed as thin layers of fine-grained or “pelitic” calciturbidites that form intercalations within the upper nodular limestone complex. These characteristic horizons are composed of material that has evidently been redeposited from the neighbouring shallow-water platform. Usually, the trigger mechanism leading to the deposition of such intercalations is interpreted as being induced by earthquakes or storms (e.g., Szulczewski 1968; Aigner 1985; Bábek *et al.* 2007) but recently Jorry *et al.* (2010) have proposed another explanation. Their analysis of the sedimentary infilling of modern basins (or atoll lagoons) that are adjacent to periodically flooded carbonate platforms has indicated that the export of carbonate material by gravity mass flows can be triggered also by a glaciostatic sea-level rise. Fast sea level rise after glacial termination produces a new accommodation space, which enables rapid platform aggradation (“catch-up stage” according to the terminology proposed for the T-factory system (*sensu* Neumann and Macintyre 1985; Schlager 2003, 2005). Simultaneously, under high dynamic conditions, the grained material is being washed off from the platform margin and deposited in the adjacent, relatively deep basins. Jorry *et al.* (2010) have proposed the term “re-flooding window” for the time, during which such a type of calciturbiditic deposition takes place. According to these authors, large redeposition of bank-derived aragonite is also associated with the flooding process. Jorry *et al.* (2010) presented a quantitative illustration of the problem and proposed a new terminology. Earlier, the connection of “high-stand shedding” with interglacial sea level rise has been discussed in numerous papers (e.g.: Droxler and Schlager 1985; Schlager *et al.* 1994), both in relation to modern reefs, as well as to fossil (e.g. Devonian) examples (Whalen *et al.* 2000, Racki *et al.* 2002).

In the case of the Late Silurian deposits investigated here, it is groundless to expect aragonite, but alternatively silt-size dolomitic grains can be found in the matrix of fine-grained peloidal packstones. This observation confirms the provenance of the peloidal material, as well as indicates a very early dolomitization of carbonate mud on the platform.

Generally, the succession investigated here can be treated as a regressive-transgressive cyclothem, with a particular phase V, which can be interpreted as a fossil record of the re-flooding processes. Additionally, it verifies the usefulness of SGR measurements in correlation of basinal and platform sequences.

Another issue worth a closer comment is connected with a rapid growth of the platform that is

dominated by peritidal facies. In the commonly accepted models, the carbonate factories are located in the subtidal zone, which supplies mud and bioclastic material to the shallower and deeper parts of the shelf (e.g., Tucker and Wright 1990; James *et al.* 2010). According to these schemes, platform progradation is the most expected process (comp. for example sections of Triassic platforms in the Dolomites: Bosellini 1984). Meanwhile, the most evident process observed in the investigated sections, is aggradation of the laminated dolomite complex, caused by a rapid rise of the sea level and an increase in accommodation space. It seems that the development of marginal platforms in the evaporitic Zechstein basins of Europe (Peryt 1984; Wagner and Peryt 1997) is a very close analogue of this situation. The continuing rapid increase in sea level has caused a retrogradational facies shift, cannibalistic disintegration of the previously deposited sediments and, finally, high dynamic deposition of the upper bio/lithoclastic limestone/dolomite complex. In this stage of the platform's development, the appearance of tidal channels (Konovka village (9) section; but also other Upper Silurian sections in Podolia (Skompski *et al.* 2008)) is a most expected feature. In consequence, it appears that the extremely shallow-water parts of the platforms, identified as tidal plains, have a surprisingly large growth potential. This conclusion seems to be underestimated in constructing most of the schemes illustrating the development of carbonate platforms.



Text-fig. 9. Sequence-stratigraphic scheme of the regressive-transgressive cyclothem between Voronovytisia and Konovka. Columns (from left): number of development phase; lithogenetic complexes; location of SGR correlation levels; sequence-stratigraphic interpretation of the investigated succession (RW – re-flooding window, FR – forced regression)

## CONCLUSIONS

Facies studies of the Upper Silurian deposits exposed along the Dnister River, combined with field spectral gamma ray (SGR) measurements made throughout the sections, allow presentation of the following general conclusions:

1. In spite of its small thickness range, the studied interval is characterized by distinct and conspicuous facies variability. The exposures are probably arranged perpendicularly to the local shoreline, and thus offer a convenient section for the analyses of bathymetrical changes.
2. Field gamma ray measurements, combined with facies studies and detailed analyses of the depositional architecture, proved to be a useful tool for creating a local stratigraphic framework. Several (seven) correlation horizons have been identified. Due to a lack of high-resolution biostratigraphy in the studied interval that could be applied to shallow water carbonate facies, and the short time span represented by the sections, the SGR measurements offered the only useful method of drawing local correlation lines. Correlated were sections developed in various facies and representing settings ranging from the inner part of a shallow water carbonate platform to its slope, through an organic buildup.
3. The two most important SGR geochemical parameters, which proved to be particularly useful in this study, are the Th/K ratio and the calculated biogenic uranium content ( $U_{\text{bio}}$ ). The Th/K ratio can serve as a proxy of thorium concentration in the terrigenous component and/or of overall changes in clay mineral composition, and thus allow short-distance correlation. The calculated biogenic uranium content ( $U_{\text{bio}}$ ) reflects the sedimentation rate, with its maxima marking condensation levels.
4. The constructed stratigraphic framework based on SGR measurements allowed interpretation of the facies evolution of the study area during the time interval analyzed. The depositional scenario can be divided into six main development stages, with the first three representing a regressive stage and the latter three a transgressive stage of the basin's history. Consecutive identified stages are manifested by: unified sedimentation on a deep sea bottom, development of the bioherm and its accompanying facies, shallowing of sedimentation and erosion of the bioherm, transgression and initiation of a new carbonate platform, and finally, retrogradational shifting of shallow water facies and the transition to another phase of a deep-sea bottom with unified sedimentation.
5. A facies record corresponding to the “re-flooding

- window” has been identified in the interval representing the initial stages of the transgression. The most characteristic features of this sedimentary phase are: accelerated growth of a tide-dominated platform, retrogradational facies shift resulting in cannibalistic destruction of older deposits, and deposition of calciturbiditic layers in the basinal area.
6. Gamma ray measurements are commonly made in deep boreholes, and are used for physical correlations of uncored parts of the sections. However, the interpretation of the data in terms of the depositional processes involved often remains dubious. Application of SGR measurements in exposed sections, and combining them with facies analyses and studies of sedimentary architecture, allowed identification of depositional sequences. The use of SGR analyses in shallow water, partly high-energy, carbonate facies, both for correlation purposes and for the identification of depositional systems, is a relatively new method and thus can serve as a reference for other studies of a similar range of facies.
  7. The Podolian exposures of the Upper Silurian offer an excellent opportunity for further studies on the response of shallow-water carbonate facies to sea-level changes.

### Acknowledgements

The studies were financed by the Polish Ministry of Education and Science Grant No N N307 013237. The authors wish to express their gratitude to Prof. Grzegorz Racki and Prof. Tadeusz Peryt, who kindly reviewed the manuscript and gave several helpful remarks.

### REFERENCES

- Abushik, A.F. and Evdokimova, I.O. 1999. Lagoonal to normal marine Late Silurian – Early Devonian ostracode assemblages of the Eurasian Arctic. *Acta Geologica Polonica*, **49**, 133–143.
- Adams, J.A.S. and Weaver, C.E. 1958. Thorium to uranium ratios as indicators of sedimentary processes; example of concept of geochemical facies. *AAPG Bulletin*, **42**, 387–430.
- Aigner, T. 1985. Storm depositional systems. *Lecture Notes in Earth Sciences*, **3**, 1–174.
- Baarli, B.G., Johnson, M.E. and Antoshkina, A.I. 2003. Silurian stratigraphy and palaeogeography of Baltica. In: E. Landing and M.E. Johnson (Eds), *Silurian Lands and Seas: paleogeography outside of Laurentia*. *New York State Museum Bulletin*, **493**, 3–34.
- Bábek, O., Prikryl, T. and Hladil, J. 2007. Progressive drowning of carbonate platform in the Moravo-Silesian Basin (Czech Republic) before the Frasnian/Famennian event: facies, compositional variations and gamma-ray spectrometry. *Facies*, **53**, 293–316.
- Bjerkéus, M. and Eriksson, M. 2001. Late Silurian reef development in the Baltic Sea. *GFF*, **123**, 169–179.
- Bosellini, A. 1984. Progradation geometries of carbonate platforms: examples from the Triassic of the Dolomites, northern Italy. *Sedimentology*, **31**, 1–24.
- Carpentier, M., Weis, D. and Chauvel, C. 2013. Large U loss during weathering of upper continental crust: the sedimentary record. *Chemical Geology*, **340**, 91–104.
- Cherns, L. 1983. The Hemse-Eke boundary: facies relationships in the Ludlow of Gotland, Sweden. *Sveriges Geol Undersökn*, **C 800**, 1–45.
- Davies, G.R. and Smith Jr, L.B. 2006. Structurally controlled hydrothermal dolomite reservoir facies: an overview. *AAPG Bulletin*, **90**, 1641–1690.
- Droxler, A.W. and Schlager, W. 1985. Glacial versus interglacial sedimentation rates and turbidite frequency in the Bahamas. *Geology*, **13**, 799–802.
- Drygant, D. 1984. Correlation and conodonts of the Silurian–Lower Devonian deposits of Volyn and Podolia. *Kiev Naukova Dumka*, 1–192. [In Russian]
- Du, X., Rate, A.W. and Gee M.A.M. 2012. Redistribution and mobilization of titanium, zirconium and thorium in an intensely weathered lateritic profile in Western Australia. *Chemical Geology*, **330–331**, 101–115.
- Durrance, E.M. 1986. Radioactivity in geology (principles and applications), 441 pp. Ellis Horwood Ltd. Halsted (Press John Wiley and Sons); Chichester.
- Dypvik, H. and Eriksen, D.O. 1983. Natural radioactivity of clastic sediments and the contributions of U, Th and K. *Journal of Petroleum Geology*, **5**, 409–416.
- Einasto, R.Z., Abushik, A.F., Kaljo, D.P., Koren', T.N., Modzalevskaya, T.L. and Nestor, H.Z. 1986. Silurian sedimentation and the fauna of the East Baltic and Podolian marginal basins: a comparison. In: D.P. Kaljo and E. Klaamann (Eds), *Theory and Practice of Ecostratigraphy*. Institute of Geology, Academy of Sciences of the Estonian SSR, Tallinn, pp. 65–72.
- Einasto, R.Z. and Radionova, M. 1988. Stromatolites and oncolites in the Ordovician and Silurian carbonate facies of Pribaltika. In: V.N. Dubotalov and T.A. Moskalenko (Eds), *Calcareous algae and stromatolites*, pp. 145–158. Nauka, Sibirskoje Otdelenije; Novosibirsk. [In Russian]
- Emery, D. and Myers, K.J. 1996. Sequence stratigraphy, 297 pp. Blackwell Science; Oxford.
- Fahraeus, L.E., Slatt, R.M. and Nowlan, G.S. 1974. Origin of carbonate pseudopellets. *Journal of Sedimentary Petrology*, **44**, 27–29.
- Feng, J-L. 2011. Trace elements in ferromanganese concretions, gibbsite spots, and the surrounding terra rossa over-

- lying dolomite: their mobilization, redistribution and fractionation. *Journal of Geochemical Exploration*, **108**, 99–111.
- Fernandez-Caliani, J.C. and Cantano, M. 2010. Intensive kaolinization during a lateritic weathering event in South-West Spain. Mineralogical and geochemical inferences from a relict paleosoil. *Catena*, **80**, 23–33.
- Flodén, T., Bjerkéus, M., Tuuling, I. and Eriksson, M. 2001. A Silurian reefal succession in the Gotland area, Baltic Sea. *GFF*, **123**, 137–152.
- Flügel, E. 2004. Microfacies of carbonate rocks – analysis, interpretation and application, 976 pp. Springer; Berlin.
- Galan, E., Fernandez-Caliani, J.C., Miras, A., Aparicio, P., and Marquez, M.G. 2007. Residence and fractionation of rare earth elements during kaolinization of alkaline peraluminous granites in NW Spain. *Clay Minerals*, **42**, 341–352.
- Gritsenko, V.P., Istchenko, A.A., Konstantinenko, L.I. and Tsegelnyuk, P.D. 1999. Animal and plant communities of Podolia. In: A.J. Boucot and J.D. Lawson (Eds), Palaeo-communities: a case study from the Silurian and Lower Devonian, pp. 462–487. Cambridge University Press; Cambridge, New York, Melbourne.
- Gu, J., Huang, Z., Fan, H., Jin, Z., Yan, Z., and Zhang, J. 2013. Mineralogy, geochemistry, and genesis of lateritic bauxite deposits in the Wuchuan-Zheng'an-Daozhen area, Northern Guizhou Province, China. *Journal of Geochemical Exploration*, **130**, 44–59.
- Handford, C.R. and Loucks, R.G. 1993. Carbonate depositional sequences and systems tracts—responses of carbonate platforms to relative sea-level change. In: R.G. Loucks and R. Sarg (Eds), Carbonate Sequence Stratigraphy; Recent Advances and Applications. *American Association of Petroleum Geologists Memoir*, **57**, 3–41.
- Hesselbo, S.P. 1996. Spectral gamma-ray logs in relation to clay mineralogy and sequence stratigraphy, Cenozoic of the Atlantic margin, offshore New Jersey. In: G.S. Mountain, K.G. Miller, P. Blum, C.W. Poag, and D.C. Twitchell (Eds), Proceedings of the Ocean Drilling Program: Scientific Results, 150. College Station, TX, 411–422.
- Hubmann, B. and Suttner, T. 2007. Siluro-Devonian Alpine reefs and pavements. In: J.J. Alvaro, M. Aretz, F. Boulvain, A. Munnecke, D. Vachard, and E. Vennin (Eds), Palaeozoic reefs and bioaccumulations: climatic and evolutionary controls. *Geological Society of London, Special Publications*, **275**, 95–107.
- Huff, W.D., Bergström, S.M. and Kolata, D.R. 2000. Silurian K-bentonites of the Dniestr Basin, Podolia, Ukraine. *Journal of the Geological Society of London*, **157**, 493–504.
- James, N.P., Kendall, A. and Pufahl, P.K. 2010. Introduction to biological and chemical sedimentary facies models. In: N.P. James and R.W. Dalrymple (Eds), Facies Models 4, pp. 323–339. The Geological Association of Canada.
- Jorry, S.J., Droxler, A.W. and Francis, J.M. 2010. Deepwater carbonate deposition in response to re-flooding of carbonate bank and atoll-tops at glacial terminations. *Quaternary Science Reviews*, **29**, 2010–2026.
- Kaljo, D. 1970. Silur Estonii (The Silurian of Estonia). Academy of Sciences of the Estonian SSR, Tallin, 343 pp. [In Russian with English abstracts]
- Kaljo, D. 1977. Facii i fauna Silura Pribaltiki (Facies and fauna of the Baltic Silurian). Academy of Sciences of the Estonian SSR, Tallin, 286 pp. [In Russian with English abstracts]
- Kaljo, D., Grytsenko, V., Martma, T. and Mõtus, M-A. 2007. Three global carbon isotope shifts in the Silurian of Podolia (Ukraine): stratigraphical implications. *Estonian Journal of Earth Sciences*, **56**, 205–220.
- Kershaw, S. 1990. Stromatoporoid palaeobiology and taphonomy in a Silurian biostrome on Gotland, Sweden. *Palaeontology*, **33**, 681–705.
- Kershaw, S., Li, Y. and Guo, L. 2007. Micritic fabric define sharp margins of Wenlock patch reefs (middle Silurian) in Gotland and England. In: J.J. Alvaro, M., Aretz, F. Boulvain, A. Munnecke, D. Vachard and E. Vennin (Eds), Palaeozoic reefs and bioaccumulations: climatic and evolutionary controls. *Geological Society of London Special Publications*, **275**, 87–94.
- Kiipli, E. and Kiipli, T. 2006. Carbonate distribution in the East Baltic deep shelf in the late Ordovician-early Silurian. *GFF*, **128**, 147–152.
- Koren', T.N., Abushik, A.F., Modzalevskaya, T.L. and Predtechensky, N.N. 1989. Podolia. In: C.H. Holland and M.G.A. Bassett (Eds), Global standard for the Silurian System. Natural Museum Wales Geological Service, **9**, 141–149.
- Laufeld, S. and Bassett, M.G. 1981. Gotland: the anatomy of a Silurian carbonate platform. *Episodes*, **2**, 23–27.
- Łuczyński, P., Skompski, S. and Kozłowski, W. 2009. Sedimentary history of Upper Silurian biostromes of Podolia (Ukraine) based on stromatoporoid morphometry. *Palaeogeography, Palaeoclimatology, Palaeoecology*, **271**, 225–239.
- Łuczyński, P., Skompski, S. and Kozłowski, W. 2014. Stromatoporoid beds and flat-pebble conglomerates interpreted as tsunami deposits in the Upper Silurian of Podolia, Ukraine. *Acta Geologica Polonica*, **64**, 261–280.
- Lüning, S. and Kolonic, S. 2003. Uranium spectral gamma-ray response as a proxy for organic richness in black shales: applicability and limitations. *Journal of Petroleum Geology*, **26**, 153–174.
- Manten, A.A. 1971. Silurian reefs of Gotland. *Developments in Sedimentology*, **13**, 271 pp. Elsevier; Amsterdam.
- McLennan, S.M., Hemming, S., McDaniel, D.K. and Hanson, G.N. 1993. Geochemical approaches to sedimentation, provenance and tectonics. In: M.J. Johnsson and A. Basu

- (Eds), Processes Controlling the Composition of Clastic Sediments, *Special Papers of the Geological Society of America*, **284**, 21–40.
- Meyers, W.J., Lu, F.H. and Zachariah, J.K. 1997. Dolomitization of mixed evaporative brines and freshwater, Upper Miocene carbonates, Nijar, Spain. *Journal of Sedimentary Research*, **67**, 898–912.
- Munnecke, A. 2007. Silurian. In: E. Vennin, M., Aretz, F., Boulvain and A. Munnecke (Eds), Facies from Palaeozoic reefs and bioaccumulations, *Mémoires du Muséum National d'Histoire Naturelle*, **195**, 113–170.
- Narkiewicz, M. 1988. Turning points in sedimentary development in the Late Devonian in southern Poland. In: N.J. McMillan, A.F. Embry and D.J. Glass (Eds), Devonian of the World, *Canadian Society of Petroleum Geologists Memoir*, **14**, 619–635.
- Narkiewicz, M. 1990. Mesogenetic dolomitization in the Givetian to Frasnian of the Holy Cross Mountains, Poland. *Bulletin of the Polish Academy of Sciences, Earth Sciences*, **38**, 101–110.
- Nestor, H. and Einasto, R. 1977. Facies sedimentary model of the Silurian Paleobaltic pericontinental basin. In: D. Kaljo (Ed.), Facies and fauna of the Baltic Silurian. Institute of Geology, Academy of Sciences of the Estonian SSR, Tallin, 17–23.
- Nestor, H. and Einasto, R. 1997. Ordovician and Silurian sedimentary basin. In: A. Raukas and A. Teedumäe (Eds), Geology and mineral resources of Estonia. Estonian Academy Publishers, Tallin, 192–195.
- Neumann, A.C. and Macintyre, I.G. 1985. Reef response of sea level rise: keep-up, catch-up or give-up. In: J.L. Gabrie, B. Toffart, and C. Salvat (Eds), Proceedings of the Fifth International Coral Reef Congress, Tahiti, 27 May – 1 June 1985, Volume 3. pp 105–110.
- Nikiforova, O.I. and Predtechensky, N.N. 1968. A guide to the geological excursion on Silurian and Lower Devonian deposits of Podolia (Middle Dniestr River). In: Proceedings of the 3<sup>rd</sup> international symposium on Silurian-Devonian boundary and Lower and Middle Devonian stratigraphy, Leningrad, pp. 1–58.
- Nikiforova, O.I., Predtechensky, N.N., Abushik, A.F., Ignatovitch, M.M., Modzalevskaya, T.L., Berger, A.Y., Novoselova, L.S. and Burkov, Y.K. 1972. Opornyj razrez silura i nizhnego devona Podolii, pp. 1–262. Nauka; Kiev
- Peryt, T.M. 1984. Sedimentation and early diagenesis of the Zechstein Limestone in western Poland. *Prace Instytutu Geologicznego*, **109**, 1–80.
- Predtechensky, N.N., Koren', T.N., Modzalevskaya, T.L., Nikiforova, O.I., Berger, A.Y. and Abushik, A.F. 1983. Cyclicity of deposition and changes of ecological assemblages of fauna in the Silurian of Podolia. *Trudy Paleontologicheskogo Instituta Akademii Nauk SSSR*, **194**, 61–74. [In Russian]
- Racki, G. 1993. Evolution of the bank to reef complex in the Devonian of the Holy Cross Mountains. *Acta Palaeontologica Polonica*, **37**, 87–182.
- Racki, G., Baliński, A., Wrona, R., Małkowski, K., Drygant, D. and Szaniawski, H. 2012. Faunal dynamics across the Silurian-Devonian positive isotope excursions ( $\delta^{13}\text{C}$ ,  $\delta^{18}\text{O}$ ) in Podolia, Ukraine: Comparative analysis of the Ireviken and Klonk events. *Acta Palaeontologica Polonica*, **57**, 795–832.
- Racki, G., Racka, M., Matyja, H. and Devleeschouwer, X. 2002. The Frasnian/Famennian boundary interval in the South Polish-Moravian shelf basins: Integrated event-stratigraphical approach. *Palaeogeography, Palaeoclimatology, Palaeoecology*, **181**, 251–297.
- Ragland, P.C., Billings, G.K. and Adams, J.A.S. 1967. Chemical fractionation and its relationship to the distribution of thorium and uranium in a zoned granite batholith. *Geochimica et Cosmochimica Acta*, **31**, 17–32.
- Ruppel, S.C. and Cander, H.S. 1988. Dolomitization of shallow-water platform carbonates by seawater and seawater-derived brines: San Andres Formation (Guadalupian), west Texas. SEPM Special Publications: Sedimentology and geochemistry of dolostones, pp. 245–262.
- Santleben, C., Munnecke, A. and Bickert, T. 2000. Development of facies and C/O-isotopes in transects through the Ludlow of Gotland: evidence for global and local influences on a shallow-marine environment. *Facies*, **43**, 1–38.
- Schlager, W. 2003. Benthic carbonate factories of the Phanerozoic. *International Journal Earth Sciences (Geologische Rundschau)*, **92**, 445–464.
- Schlager, W. 2005. Carbonate sedimentology and sequence stratigraphy. *Concepts in Sedimentology and Paleontology*, **8**, 1–200.
- Schlager, W., Reimer, J. and Droxler, A. 1994. Highstand shedding of carbonate platforms. *Journal of Sedimentary Research*, **B64**, 270–281.
- Skompski, S., Łuczynski, P., Drygant, D. and Kozłowski, W. 2006. Silurian of Podolia; Kamieniec Podolski–Kubachivka Quarry; Skala Podolska–Bridok Quarry. In: A. Wysocka and M. Jasionowski (Eds), II Polish Sedimentological Conference Guide. Instytut Geologii Podstawowej UW, Warszawa, 93–108. [In Polish]
- Skompski, S., Łuczynski, P., Drygant, D. and Kozłowski, W. 2008. High-energy sedimentary events in lagoonal successions of the Upper Silurian of Podolia, Ukraine. *Facies*, **54**, 277–296.
- Spirakis, C.S. 1996. The roles of organic matter in the formation of uranium deposits in sedimentary rocks. *Ore Geology Reviews*, **11**, 53–69.
- Środoń, J., Paszkowski, M., Drygant, D., Anczkiewicz, A. and Banaś, M. 2013. Thermal history of lower Paleozoic rocks on the Peri-Tornquist margin of the East European Craton (Podolia, Ukraine) inferred from combined XRD, K-Ar,

- and aft data. *Clays and Clay Minerals*, **61**, 107–132.
- Szulczewski, M. 1968. Slump structures and turbidites in Upper Devonian limestones of the Holy Cross Mts. *Acta Geologica Polonica*, **18**, 303–330.
- Taboada, T., Martinez-Cortizas, A., Garcia, C. and Garcia-Rodeja, E. 2006. Uranium and thorium in weathering and pedogenetic profiles developed on granitic rocks from NW Spain. *Science of the Total Environment*, **356**, 192–206.
- Tsegelnjuk, P.D. 1974. Dnistrovskij opornyj razriz siluru. In: D.E. Aizenverg (Ed), *Stratigrafija URSR – Silur*, **6**, 63–110. Naukova Dumka; Kiev.
- Tsegelnjuk, P.D., Gritsenko, V.P., Konstantinenko, L., Ishchenko, A.A., Abushik, A.F., Bogoyavlenskaya, O.V., Drygant, D.M., Zaika-Novatsky, V.S., Kadlets, N.M., Kiselev, G.N. and Sytova, V.A. 1983. The Silurian of Podolia. The guide to excursion, 224 pp. Naukova Dumka; Kiev. [In Russian]
- Tucker, M. and Wright, V.P. 1990. *Carbonate Sedimentology*, 482 pp. Blackwell Scientific Publications; Oxford.
- Tuuling, I. and Floden, T. 2011. Seismic stratigraphy, architecture and outcrop pattern of the Wenlock-Pridoli sequence offshore Saaremaa, Baltic Sea. *Marine Geology*, **281**, 14–26.
- Vannier, J., Wang, S.Q. and Coen, M. 2001. Leperditicopid arthropods (Ordovician-Late Devonian): functional morphology and ecological range. *Journal of Palaeontology*, **75**, 75–95.
- Wagner, R. and Peryt, T.M. 1997. Possibility of sequence stratigraphic subdivision of the Zechstein in the Polish Basin. *Kwartalnik Geologiczny*, **41**, 457–474.
- Ward, W.C. and Halley, R.B. 1985. Dolomitization in a mixing zone of near-seawater compensation, Late Pleistocene, North-eastern Yucatan. *Journal of Sedimentary Petrology*, **55**, 407–420.
- Watkins, R. 1992. Paleocology of a low-diversity Silurian community from the Tofta Beds of Gotland. *Paläontologische Zeitschrift*, **66**, 405–413.
- Whalen, M.T., Eberli, G.P., Van Buchem, F.S.P., Mountjoy, E.W. and Homewood, P.W. 2000. Bypass margins, basin-restricted wedges, and platform-to-basin correlation, Upper Devonian, Canadian Rocky Mountains: Implications for sequence stratigraphy of carbonate platform systems. *Journal of Sedimentary Research*, **70**, 913–936.
- Wilson, R.C. 1967. Particle nomenclature in carbonate sediments. *Neues Jahrbuch für Geologie und Paläontologie, Monatshefte*, 498–510.

*Manuscript submitted: 15<sup>th</sup> April 2015*

*Revised version accepted: 15<sup>th</sup> August 2015*